Intra- and inter-specific variation in root mechanical traits for twelve herbaceous plants and their link with the root economics space

Zhun Mao, Catherine Roumet, Lorenzo Rossi, Luis Merino-Martín, Jérôme Nespoulous, Olivier Taugourdeau, Hassan Boukcim, Stéphane Fourtier, Maria del Rey Granado, Merlin Ramel, et al.

Intra- and inter-specific variation in root mechanical traits for twelve herbaceous plants and their link with the root economics space

Zhun Mao, Catherine Roumet, Lorenzo M. W. Rossi, Luis Merino-Martín, Jérôme Nespoulous, Olivier Taugourdeau, Hassan Boukcim, Stéphane Fourtier, Maria Del Rey-Granado, Merlin Ramel, Kang Ji, Juan Zuo, Nathalie Fromin, Alexia Stokes, Florian Fort

Abstract

Root mechanical traits, including tensile strength (T_r), tensile strain (ε_r), modulus of elasticity (E_r) and tensile toughness (W_r), play a key role in plant functioning (e.g., anchorage and stem stability). Yet, their variability and their relationships with other root traits are poorly known. Here, we characterize T_r, ε_r, E_r and W_r at both intra- and interspecific levels and examine how they covary with other root traits related to root economics space (RES). We used twelve herbaceous species from contrasting taxonomical families grown in controlled plein-air conditions. For each species, we excavated root systems and measured morphological and chemical traits and mechanical traits at two locations (*proximal* versus *distal*) for two root types (*absorptive* versus *transport* roots). Transport roots tended to show higher mechanical trait values than absorptive roots, especially for ε_r, while the location where the root was sampled showed a limited effect on root mechanics. The five monocots (Poaceae species) had higher mechanical traits than the seven dicots (including five Fabaceae species) except for E_r. Root mechanical traits covaried positively and were strongly positively correlated with specific root length, i.e., a trait related to soil exploration strategy, and negatively with root diameter and root tissue density, i.e. a trait related to root life span. We demonstrate the important role of species category and root type in governing mechanical trait variation at both intra- and inter-specific levels. Our results can be regarded as the first evidence of the link between root mechanical robustness and the RES through a strong association with the 'do-it-yourself' soil exploration strategy.

Key words: mechanical traits, tensile strength, modulus of elasticity, tensile strain, toughness, economics spectrum, root economics space.

1 INTRODUCTION

Mechanical properties differ throughout plant organs and impact growth, defence, survival and reproduction (Wright and Westoby 2002; Read and Stokes 2006). For example, mechanical traits of roots strongly influence anchorage and the capacity of a root of root to penetrate soil during resource scavenging (Chimungu et al. 2015; Loades et al. 2015; Niklas et al. 2002; Stokes et al. 2009). However, root mechanical traits have been studied little, especially in herbaceous species, and our knowledge of the underlying mechanisms impacting the resistance of roots to loading forces, both within and across species, remains scarce.

Roots of herbaceous species need to avoid uprooting from e.g. animal grazers and soil displacement (Stokes et al. 2009). Resistance to uprooting depends on the shape of the root system and root mechanical properties. As a root is exposed to various forces during uprooting, it will stretch, then either slip through the soil or break (Waldron and Dakessian 1981). Four representative mechanical traits can be cited to describe the mechanical quality of root tissue as a material in a uprooting processes (Table 1): (i) tensile strength (T_r) is the maximum force required, per cross-sectional area of the root, to cause failure in tension. Failure can occur through either breakage or permanent deformation. T_r is the mechanical trait most frequently measured on individual roots (Freschet et al. 2021) and a higher value of T_r means root tissue (not an individual root) is stronger. (ii) Longitudinal modulus of elasticity (E_r) is the resistance to being deformed elastically in tension, but without failure occurring. E_r measures tensile stiffness of root tissue. A higher value of E_r means that root tissue is more elastic or stiffer, and has a better capacity to withstand tension without undergoing permanent deformation, improving plant anchorage. (iii) Tensile strain (ε_r) is the relative longitudinal extension when failure occurs. During uprooting, root tissue with a high strain value can better help a root remain anchored in soil, even after soil failure has occurred, holding vegetation in place and reducing soil movement. (iv) Tensile toughness (W_r) is the energy (or work) required per unit

root volume to cause failure in tension. Toughness helps protect against disturbance and so enhances organ lifespan (Read and Stokes 2006). As well as describing how roots are anchored in soil, and how they fail during loading, these traits are also key parameters in root reinforcement and slope stability models that assess the contribution of vegetation for protecting against shallow landslides (Mao 2022).

At the intraspecific level, root mechanical traits are highly variable and are usually characterized as a function of root diameter (de Baets et al. 2008; Burylo et al. 2011; Ghestem et al. 2014; Ji et al. 2020). For example, many studies have shown that a negative power law relationship occurs between root strength and diameter (Genet et al. 2005; Fan and Su 2008; Mao et al. 2012; Ghestem et al. 2014; Ji et al. 2020; Meijer 2021), suggesting that finer roots are stronger as a material than coarser roots. This phenomenon has been attributed to differences in root structure, with thinner roots possessing more cellulose per dry mass than coarser roots (Zhang et al. 2014; Zhu et al. 2020). Also, differences in root anatomy occur, with thinner roots often possessing a higher proportion of lignified stele (Kong et al. 2014) and a lower proportion of mechanically weak cortex (Mao et al. 2018). However, a number of recent studies revealed that root diameter is not an ideal predictor of mechanical traits. For example, according to species, the relationship between strength and diameter is either positive, null or negative (Boldrin et al. 2017; 2018; Mao et al. 2018). Root age or root location (e.g. sampling distance from root tip; Dumlao et al. 2015; Loades et al. 2015; Boldrin et al. 2021), water status (Boldrin et al. 2018; Ekeoma et al. 2021), type (nodal, seminal or lateral; Loades et al. 2015), anatomy (Chimungu et al. 2015; Mao et al. 2018) and topological order (Mao et al. 2018) have all been found to better explain mechanical trait variation than diameter alone. Roots of most plant species can be classed into (i) *absorptive* roots, which represent the most distal roots dedicated to the acquisition and uptake of resources, and (ii) *transport* roots, that occur at higher branching orders and have mainly transport and mechanical functions (McCormack et al. 2015).

Mao et al. (2018) examined the intraspecific variation of mechanical traits as a function of topological order for four tropical tree species and showed that lower-order *absorptive* roots were weaker and less stiff, but could extend further before failure, compared to higher-order *transport* roots. Therefore, root mechanical quality contributes to the shift from acquisition to transport functions .In addition,, the effect of root location (*proximal* vs *distal*) within *absorptive* and *transport* roots on mechanical properties (Fig. 1) is poorly known, even though it may impact anchorage capacity.

Mechanicals traits of individual roots have mostly been studied in an attempt to find species with strong roots that can resist uprooting and substrate mass movement (Ghestem et al. 2014; Boldrin et al. 2017). However, the drivers of interspecific variability are poorly understood (Freschet et al. 2021) and can result from inherent structural and anatomical design , as well as differences in chemical make-up of cell tissue. Compared to studies on traits aboveground, there is a lack of comparative studies investigating the relationships between root mechanical traits and other morphological and chemical traits (Freschet et al. 2021). For example, a global pattern of interspecific mechanical trait variation in leaves has showed that leaf strength (work to shear failure) was strongly and positively correlated with leaf mass area, thickness, tissue density and life span (Wright and Westoby 2002; Onoda et al. 2011; Méndez-Alonzo et al. 2013). These relationships show that leaf strength is part of the leaf economics spectrum highlighting a trade-off between carbon and nutrient acquisition and conservation (Wright et al. 2004). To our best knowledge, whether such patterns also occur in root system has not been investigated. Based on a database of more than 1800 species worldwide, Bergmann et al. (2020) demonstrated that fine roots traits (classed as $\leq$ 2.0 mm) covaried in a two-dimensional space, namely the root economics space (RES). One axis, the conservation gradient, represents a trade-off between high metabolic activity, with high root nitrogen concentration (RNC) and an investment in long lived structural tissues, i.e., high root tissue density (RTD). The other axis is called the

collaboration gradient, and relates to soil exploration strategies. This axis represents a trade-off between (i) a "do-it-yourself" strategy, where soil exploration and exploitation is achieved by roots with high specific root length (SRL) and (ii) an "outsourcing" strategy, where resource acquisition is delegated to mycorrhizal fungi hosted in thick roots, i.e. high mean root diameter (RD). This framework considered morphological and chemical, traits, but did not integrated mechanical traits for the simple reason that these traits are not available in root trait databases (Iversen et al. 2017; Guerrero-Ramírez et al. 2021). Nevertheless, as for global patterns of leaf mechanical properties (Onoda et al. 2011), fine root strength and other mechanical traits are expected to be an integral part of the RES. The few studies examining relationships among mechanical, morphological and chemical traits suggest that mechanical traits are associated with the conservation axis, because tensile strength and/or stiffness are positively associated with RTD (Yang et al. 2016; Boldrin et al. 2018), cellulose concentration (Genet et al. 2005), lignin concentration (Zhang et al. 2014; Zhu et al. 2020; Hathaway and Penny 1975) and/or lignin to cellulose ratio (Hathaway and Penny 1975; Zhang et al. 2014) and are negatively correlated with soluble sugar concentration (Genet et al. 2011). However, these studies mostly focused on woody species and measured on different root types (with diameters ranging from 0.1 to 10.0 mm). It remains unclear whether such patterns (i) are consistent within *absorptive* and *transport* fine roots, (ii) are consistent for mechanical traits other than tensile strength and stiffness (e.g., toughness and strain) and (iii) can be extrapolated to herbaceous species belonging to different species categories (monocots versus dicots).

Monocot root systems differ from dicots in terms of architecture (Pagès 2016) and generally have a fibrous root system with many root axes lacking secondary xylem in the stele. Dicots often have a well-anchored taproot and roots possessing secondary tissues. Monocot roots were usually thinner with low tissue density, RNC and cellulose concentration, but higher SRL and C:N ratio than dicots (Roumet et al. 2016; Freschet et al. 2017; Rossi et al. 2020). In addition,

monocot leaves are generally more resistant to tearing than dicot leaves (Onoda et al. 2011). Altogether, this suggest that roots of monocot roots are stronger and tougher than dicot roots, but a comparative study of plant species grown in the same conditions has not been performed.

In this study, using twelve herbaceous species from contrasting taxonomical families and species categories (monocots versus dicots), we aim at characterizing the intra- and interspecific variations of four root mechanical traits, including tensile strength (T_r); tensile strain (ε_r); modulus of elasticity (E_r) and tensile toughness (W_r), and examine how these mechanical traits covary with root morphological and chemical traits related to root economics. For each species, we measured mechanical traits at two locations (*proximal* versus *distal*) for two root types (*absorptive* versus *transport*), using a standardized protocol. We hypothesize that: (H1) at the intraspecific level, root diameter, type (*absorptive* versus *transport* roots) and location (*proximal* versus *distal*) contribute to explain variations in mechanical traits; (H2) at the interspecific scale, root mechanical traits are part of the root economics space. In particular, we expect that species with thinner roots and high SRL and/or with more recalcitrant tissues (i.e., low RNC, but high RTD and C:N ratio) have stronger, stiffer and tougher root tissues that are capable of being deformed before failure. Finally, we hypothesize that: (H3) monocots with high SRL and thinner roots have higher mechanical quality than dicots.

2 MATERIALS AND METHODS

2.1 Species and experimental setup

The experiment was conducted on twelve perennial herbaceous species, including five monocots and seven dicots belonging to four botanical families (Table 2). These species were grown at the CEFE experimental garden (Montpellier, France; 43° 38' 20" N, 3° 51' 51" E). The climate is Mediterranean subhumid (Daget 1977) with high sunshine hours, warm and dry summer (with mean daily maximum temperature in July; 24 °C) and cool to cold winters (with

mean daily minimum temperature in January; 7 °C). During the experiment, from October 2016 (seed-sowing) to July 2017 (plant harvesting), a weather station in the experimental garden measured the maximum, mean and minimum air temperatures, which were 30 °C, 13 °C and -0.4 °C, respectively, and the cumulative precipitation, which was 349 mm (Rossi et al. 2020).

This study was part of a larger program on the revegetation of embankments in southern France (Rossi et al., 2020). Therefore, the twelve herbaceous plant species were grown as monocultures in three replicate steel boxes (0.7 m in length × 0.7 m width × 0.3 m depth) and positioned at a slight inclined angle (20° relative to horizon) for mimicking a road embankment, where these species are commonly found. Each species was sown in October 2016 in lines, with both intra-row and inter-row spaces between two plants fixed to 75 mm, resulting in a plant density of 155 plants per m^2. The soil used for the cultivation was excavated at Villefort, France (44° 26' 25" N, 3°55' 58" E) and was a sandy loam with 63% sand, 26% silt and 11 % clay, respectively. The concentrations of total organic C, total N, and Olsen P were 16.90 g kg^{-1}, 1.36 g kg^{-1} and 0.069 g kg^{-1}, respectively. The pH was 7.06 and cation-exchange capacity was 7.98 cmol kg^{-1}. All the treatments, from soil sieving, box filling and *Rhizobium* inoculation for soil, to daily irrigation with programmed sprinklers, weeding (manually, every week) and mowing (every four months) for plants, were identically applied to all the boxes (Rossi et al. 2020).

2.2 Root sampling and measurement for root morphological and chemical traits

For each box (i.e., three replicates per species), a cylinder soil core (75 mm diameter, 200 mm depth), centered on one individual plant per species was collected in July 2017. Roots were washed under water and sorted into two root types: *absorptive* roots, typically the first, second and third root orders (defined as the most distal root orders), and *transport* roots, that were higher order roots (all orders above third order roots, following McCormack et al. (2015). By

default, root topological orders in this study refer to those counted by the morphometric root classification method, see Freschet et al. (2021).

For each species, two subsamples of absorptive and of transport roots were used for measurements of root morphology and chemical composition. For morphological traits, roots were stained in methyl violet solution (0.5 g L^{-1}), scanned at 800 dpi (Epson Expression 1680, Canada), oven dried at 60 °C for 3 days and weighed to obtain dry root mass. The scanned images were analyzed via the software Winrhizo Pro (Regent Instruments, Quebec, Canada) to obtain the root length, root volume in different diameter classes (from 0 to 2 mm diameter with a 0.1 mm interval) and mean root diameter (RD, in mm) was calculated for absorptive and transport roots as the weighted average of the median of each diameter class by the length of the roots in each class. Specific root length (SRL, in m g^{-1}) was calculated as the ratio between root length and dry root mass. Root tissue density (RTD, in g cm^{-3}) was calculated as the ratio between root dry mass and root volume. For each root type, root carbon (C) and nitrogen (N) concentrations were measured with another subsample of roots using an elemental analyser (CHN model EA 1108; Carlo Erba Instruments, Milan, Italy) so that root carbon to nitrogen ratio (i.e., C:N ratio) could be estimated. Mean values of the above traits for are summarized in Table S1.

2.3 Root sampling for root mechanical traits

Unlike the above root morphological and chemical traits, root mechanical traits were measured per root individual rather than on a sample of several roots. Because of the destructive nature of the sampling procedure that would affect other root trait or soil feature measurements, for each species, we randomly selected one of the three replicate boxes for sampling roots (one box per species). For each selected box, a soil monolith (18 cm (length) × 18 cm (width) × 30 cm (depth)) was excavated in the middle of the box so that multiple (≥5) plant individuals were

sampled. Each soil monolith was then transferred into a container filled with water. Using a shower nozzle, soil was removed without damaging roots. Then, we placed the mass of roots in a tray filled with clean water and carefully selected five entire root branches (i.e., five replicates) in a random manner. Root branch selection at the same location of the plants was avoided. Each selected root branch started from either a root connected to a taproot (for dicots; i.e., the 1st order lateral of a basal root according to the developmental root classification approach (Freschet et al. 2021) or a root from the base of a culm (for monocots) (Fig. 1). This method ensured that the lateral root branches of different species followed the same selection criterion and so facilitated interspecific comparison. For each species, each of the five root branches was carefully removed from the rest of root system, using a knife. In each root branch, we defined four categories of root segments (Fig. 1): (i) a segment at the proximal part of the root originating from the taproot (in dicots) or the base of a culm (in monocots) (*Transport – Proximal*); (ii) a segment from the distal part of the same root (*Transport – Distal*); (iii) a proximal segment from a daughter root (*Absorptive – Proximal*) and (iv) a distal segment from the lower part of the same root (*Absorptive – Distal*). We carried out a visual check and used Fitter (1982)'s morphometric root classification method (Freschet et al., 2021) for assessing topological order, counting from the distal segments to ensure that samples (1) and (2) were *transport* roots with root orders >3 and whose main function is supposed to be transport and anchorage, and samples (3) and (4) were *absorptive* roots with root orders ≤3 whose main function is supposed to be the absorption of water and nutrients. Based on an anatomical approaches over 34 herbaceous species, Zhou et al. (2022) found that root function shifted from absorption to transport with increase root order for both monocots and dicots, although the proportion between cortex and stele differed between the two species categories. In this paper, we need to apply the same criteria when comparing roots of different species. That is why the

categorization between 1–3rd and 4–5th was applied for all the species regardless of category (monocot versus dicot).

2.4 Root mechanical test and trait estimation

Procedures of root mechanical test and trait estimation generally followed the protocol used in Mao et al. (2018). Each of the selected root segments (N = 20 per species: 2 root types × 2 positions × 5 replicate branches) was carefully cut for the measurement of diameter using a microscope. We took three high resolution images at three different locations: in the middle and near each end of the root segment. For each image, root diameter was measured twice at two randomly selected locations along the root segment. Consequently, we obtained six measurements of root diameter per sample. We used the mean of the six diameters (d, in mm) in the calculation of T_r, E_r and W_r.

An In-Spec 2200 BT (Instron© Corporation) tensile testing machine was used for mechanical tests. A force transducer with a maximum capacity of 125 N was used and each root segment was placed into vertically aligned rubber-lined jaws that were manually tightened. Roots with diameter > 1.0 mm were fixed using strips of sandpaper and cyanoacrylate adhesive to prevent slippage (Giadrossich et al. 2017). Roots that slipped during a test were discarded and all tests where roots broke in between the jaws were considered as successful (the success rate was >80%; Table 2).

For each root segment tested, the initial gauge length (i.e. distance between the two grips, L_0, in mm) was measured using Vernier callipers and ensured to be at least 20 times the diameter of the root. The crosshead speed was fixed at 5.0 mm min^{-1}. After a test started, the time-dependant tensile load, or force (F, in N) and stress (σ, defined as the standardized tensile load by root cross-sectional area, in MPa), displacement (L, defined as the absolute root deformation, in mm) and strain (ε, defined as the relative deformation to the initial length L_0, in %) were

measured automatically until the occurrence of root failure. For each root segment, the curve of F against L can be converted to the curve of σ against ε which shares the same shape to the former (Table 1). Based on both curves, five parameters were estimated (Table 1), including tensile load required to cause root failure (F_r; in N), root tensile strength (T_r; in MPa), ;root tensile strain (ε_r; in %), root modulus of elasticity in the longitudinal direction (E_r, *idem.* to MoE_L in Freschet et al. (2021); in MPa) and root tensile toughness (W_r; in MJ m^{-3}).

Mathematically, E_r and W_r could be retrieved by performing a derivative and an integral over a polynomial equation fitted curve of σ against ε between the start of the test and the failure of the root segment, respectively. F_r is closely dependent on root diameter (Table S2), as a thicker sample of the same material requires a higher force for rupture (Mao et al. 2018). We observed strong and positive increases in F_r with increasing diameter and their relationships were well fitted by a power law function (with adjusted R^2 = 0.16–0.99; Fig. S1; see also Section 2.5). Unlike F_r, all the other metrics (T_r, ε_r, E_r and W_r) are standardized by root size either root cross-sectional area ($0.25\pi d^2$) or initial length (L_0) or both and reflect the intrinsic quality of root material (Table 1). Hereafter, root mechanical traits only refer to T_r, ε_r, E_r and W_r in the Results and Discussion sections. It is to be noted that W_r of this study slightly differs from that in Ji et al. (2021) that did not standardize the energy-based metric by root initial length (L_0).

2.5 Statistical analyses

At the intraspecific level, we performed power law regression fits to explore the relationships between root mechanical parameter and root diameter for each species (Cohen et al. 2011; Meijer 2021):

$$Y_r = Ad^B \quad \text{(Eq. 1)}$$

Where, Y_r denotes a root mechanical parameter (e.g., F_r, T_r, ε_r, E_r or W_r); d denotes root diameter of a single root (mm); A (multiplier) and B (exponent) are the two parameters to calibrate. The power law regression is negative when $B < 0$ and positive when $B > 0$, i.e. roots of larger diameters have respectively a lower ($B < 0$) or larger mechanical traits ($B > 0$). When B is not significant from zero, it signifies that mechanical traits varies little as a function of diameter. Then, for each species, we performed the Student's t-test to examine the effect of root type (*transport* roots versus *absorptive* roots) and root position (*proximal* versus *distal*).

At the interspecific level, we first performed the Student's t-tests to check the effect of species category (monocot versus dicot). The tests were applied to data of all species and for each of the combinations of root type (*transport* versus *absorptive*) and location (*proximal* versus *distal*). We additionally performed analyses of variance (ANOVA) and Post-hoc tests (i.e., Tukey Honestly Significant Difference (HSD) tests) to discriminate between root mechanical traits among species for each root type and location.

We performed two principal component analyses (PCA) to explore multiple-trait relationships for absorptive and transport roots, respectively. We used averaged traits of the four structural traits (SRL, RNC, RTD and RD) and the four mechanical traits (T_r, ε_r, E_r and W_r) per root type. Before a PCA, traits were standardized using the zero-mean approach. Facilitating visual data interpretation, we used the convex hull polygon algorithm to describe the occupation of the data points belonging to a category (monocots versus dicots). Besides PCA, we used scatter plots to illustrate the relationships between the four mechanical traits (T_r, ε_r, E_r and W_r) and the four structural traits (SRL, RNC, RTD and RD) as a function of root type and species category, for which linear regressions were performed.

We also used Pearson's correlation for bivariate correlations and before the test, traits were log-transformed to minimize the effect of nonlinearity. Besides the trait-value based correlation, we

296 also performed Pearson's correlation using phylogenetic-independent contrasts (PICs) that take
297 into account the phylogenetic nonindependence of the species during the evolutionary history
298 (Felsenstein 1985). We performed a Mantel test between trait-based and PIC-based correlation
299 matrices to examine whether correlation patterns differ when including PICs.

300 All statistical analyses were performed using R 4.1.0 (R Core Team, 2021). PCA was performed
301 with the R package "vegan" (Oksanen et al., 2020). Tukey HSD test was performed with the
302 help of the R package "multcompView" (Graves et al., 2015). Pearson's correlation was
303 performed with the R package "Hmisc" (Harrell Jr, 2019). PICs were calculated using the R
304 package "APE" (Paradis et al. 2004) based on the species' phylogenic relationship generated
305 by the R package "V.PhyloMaker" (Jin and Qian 2019).

306 **3 RESULTS**

307 ***3.1 Intraspecific variation in root mechanical traits***

308 Relationships between any mechanical trait and root diameter were poorly captured by the
309 power law function that is usually used to describe such relationships (Meijer 2021) (Figs. 2, 3,
310 4 and 5). The best fit was found for tensile strain (ε_r) (with adjusted R^2 = 0.14–0.65 Fig. 3),
311 whereas both tensile strength (T_r) and modulus of elasticity (E_r) showed either positive,
312 negative or non-significant relationships with root diameter depending on species (Figs. 2 and
313 4). For most species, the exponent parameter (B) was not significantly different from zero (11
314 out of 12 species for T_r and 9 out of 12 species for E_r) (Figs. 2 and 4), but an opposite pattern
315 was found for ε_r (10 out of 12 species having B significantly higher than zero) (Fig. 3).
316 Toughness (W_r) showed either no relationship (i.e. B not significantly different from zero for 9
317 out of 12 species) or a slightly positive relationship (i.e. B significantly different from zero for
318 3 out of 12 species) with increasing root diameter (Fig. 5).

319 For 10 out of the 12 species ε_r was significantly higher in *transport* roots than in *absorptive*
320 roots (Table 3; Fig. 3). More than half the species did not show any differences in T_r, E_r and W_r
321 between *transport* and *absorptive* roots, although a tendency toward higher values in *transport*
322 roots was observed (Table 3; Figs. 2, 4 and 5).

323 Compared to root type (*transport* versus *absorptive*), root location (*proximal* versus *distal*) did
324 not strongly impact mechanical traits, except in certain species (Table 3). This result is
325 especially true for *absorptive* roots of *M. sativa* and for *transport roots* of *P. lanceolata* and *L.*
326 *corniculatus* which were the only species showing significant differences in mechanical traits
327 between *proximal* and *distal* roots (Table 3).

328 ***3.2 Interspecific variation in root mechanical traits***

For any mechanical trait of either *transport* or *absorptive* roots, the effect of species was always significant (ANOVA; Table 3). The first two species that possessed the highest values were always from the Poaceae family, whereas mechanical traits of the remaining 10 species were not significantly different regardless of root type or location (Table 3).

Significant effects of species category (monocots versus dicots) on mechanical traits were found for most combinations of root type and location (Student's t-tests; Fig. 6). For both *absorptive* and *transport* roots, the seven dicots had significantly lower T_r, ε_r and W_r compared to the five monocots, whereas E_r did not differ between monocots and dicots (Fig. 6).

3.3 Relationships among mechanical, morphological and chemical traits for absorptive and transport roots

The Mantel *r* of 0.905 with P <0.001*** showed that there was strong positive correlation between the trait-based and PIC-based matrices, indicating the generally constant tendencies of trait-trait relationships between the trait-based and PIC-based matrices. Considering or not the effect of phylogeny changed little the correlations among root mechanical traits, but did affect correlations between root economics-related morphological and chemical traits and between mechanical traits and economics-related traits (Table 4). Hereafter, results of trait-based Pearson' correlation are referred to by default. For both *transport* and *absorptive* roots, in general, the four mechanical traits covaried positively and they were all positively correlated with SRL and negatively correlated with RD (Table 4). RNC was not correlated with T_r and E_r, but was negatively corelated with ε_r and weakly and negatively correlated with W_r (only for *transport* roots) (Table 4). The correlation between RTD and ε_r was negative for *transport* roots, but not significant for *absorptive* roots (Table 4). The correlation between RTD and T_r and E_r was not significant for *transport* roots but was negative for *absorptive* roots (Table 4). Results

352 from Pearson's correlations were in good accordance with those from linear regressions (Fig.
353 S3), despite some disparities of significance due to different methods.

354 In both PCAs, the first two axes explained >75% and >80% of the variation among all traits for
355 *transport* roots and *absorptive* roots, respectively (Fig. 7). In particular, both of the first axes
356 explained more than 65% of the variation. Trait coordination of *transport* and *absorptive* roots
357 showed some consistency along their first axes, despite pronounced differences along the
358 second axes. For both root categories, the first PCA axis was driven by RD toward the positive
359 direction, and by SRL toward the negative direction (Fig. 7). For *absorptive* roots, the second
360 axis was associated with RNC at one end and with RTD at the other end. In contrast, for
361 *transport* roots, RTD and RNC were strongly associated with RD along the first axis.

362 For both root types, all mechanical traits tended to be associated with the first axis toward the
363 negative direction (i.e., in the same direction as SRL but opposite to RD). The second axis
364 slightly distinguished ε_r (toward the positive direction) from T_r, E_r and W_r for *transport* roots
365 (Fig. 7b) and distinguished E_r (toward the negative direction) from ε_r for *absorptive* roots (Fig.
366 7a). The quasi-non-overlapped convex hull polygons in both PCAs indicated that the five
367 monocots were strongly discriminated from the seven dicots (Fig. 7). The monocots were
368 mainly associated with higher SRL, C:N ratio and higher T_r, ε_r, E_r and W_r, but lower RD, RNC
369 and RTD (Table S1; Fig. 7). Scatter plots with linear regressions between mechanical and
370 economics-related traits showed that data points were more segregated by root type (*absorptive*
371 versus *transport*) rather than species category (monocot versus dicot; Fig. S3).

372

4 DISCUSSION

We found that along with root diameter, root type (*transport* versus *absorptive*), but not root location (*proximal* versus *distal*), could best explain the variation in mechanical traits at intraspecific levels, thus partially rejecting our hypothesis H1. In line with our H2, we showed that a strong coordination existed between mechanical traits and several economics-related morphological and chemical traits. As expected, in both *absorptive* and *transport* roots, thin roots with high SRL were stronger and tougher, but surprisingly, also had lower RTD. Then, in line with our H3, we showed that species category (monocots versus dicots), significantly affected mechanical traits: monocots had stronger (i.e., higher T_r), tougher roots (i.e., higher W_r) roots that deformed more under loading (i.e., higher ε_r) than dicots, but stiffness (E_r) was not altered.

4.1 Intraspecific variation in mechanical traits is driven by root type, not by root location (H1)

At the intraspecific level for most species (nine out of twelve), we showed that strength (T_r), stiffness (E_r) and toughness (W_r) did not vary significantly with root diameter and only in a few species (two to six) were *transport* roots stronger, stiffer and tougher than the thinner *absorptive* roots. These results contrast with most previous studies showing that T_r and E_r of roots decrease with increasing diameter, not only in herbaceous species, but also in shrubs and trees (Fan and Su 2008; Mao et al. 2012; Loades et al. 2015). The absence of a relationship between T_r and diameter is however not so surprising given the number of factors other than root diameter controlling root strength, such as root age (Boldrin et al. 2021), water content (Ekeoma et al. 2021), topological order and anatomy (Mao et al. 2018). In order to avoid all these confounding effects we normalized root sampling: (i) roots were sampled according to root type and location within the root system, (ii) >99 % of roots had a diameter of <2 mm (iii) roots were fully

hydrated to avoid drying that influence root diameter and mechanical properties and (iv) in each sampling population, equal or quasi-equal numbers of replicates were ensured (Table 2). This procedure avoided a major pitfall in many previous studies, where root samples are arbitrarily picked along a given diameter span, resulting in an over-sampling of the more abundant very fine roots, or sampling of mixtures of *transport* and *absorptive* roots. Root strength and stiffness are highly variable in very fine roots, often displaying extreme values (Mao et al. 2018), and biasing mean results. Additionally, including thicker (2 – 8 mm) and highly lignified roots (see Genet et al. 2005 and de Baets et al. 2008) may also bias results, as root mechanical integrity can be compromised due to the presence of material defects in cell wall microstructure. Material defects can non-linearly deteriorate the mechanical quality of a material (Timoshenko 1956) and are the result of anomalies in cell wall differentiation, imperfections in cell adhesion or damage caused as, for example, a root grows through soil with its multitude of diverse physical properties and root herbivores (Schumacher et al., 2021; Williamson and Gleason, 2003).

Root tensile strain significantly increased with increasing root diameter for ten out of the twelve species, but it was the only trait calculated using root length measurements before and after the mechanical test (Table 1), therefore the influence of mechanical defects will have a smaller effect on results compared to root thickness.

Transport roots were thicker and able to deform further (i.e., higher ε_r) than *absorptive* roots and this result was consistent for ten out of twelve species (Table 3; Fig. 3). Differences between *transport* and *absorptive* roots likely result from internal anatomical design. Compared to *transport* roots, *absorptive* roots (i.e. the lower root orders) have a higher cortex:stele surface area ratio and little or no secondary thickening (i.e., low suberisation and lignification) (McCormack et al. 2015). Compared to the lignified stele, cortex is usually much weaker mechanically due to its higher content of large, water-filled and thin-walled parenchyma cells (Ekeoma et al. 2021). In addition, *absorptive* roots are generally ephemeral and so may not

require a major investment in mechanical quality, whereas *transport* roots possess both structural and transport functions and so their high mechanical resistance to failure as shown in this study shall help enhance persistence and life span in soil.

4.2 Interspecific variation of mechanical traits: strong coordination with morphological traits (H2)

At the interspecific level, as expected but in contrast to results found at the intraspecific level, mechanical traits (except for stiffness) were negatively correlated with root diameter. The best predictor of mechanical traits was SRL, for both *absorptive* and *transport* roots.

In *absorptive* roots, the PCA performed with the four mechanical traits and the four core root traits of the root economics space (RES) (SRL, RD, RTD and RNC; Bergmann et al. 2021) supports the RES framework and demonstrates that mechanical traits are an integral part of the RES. The four fundamental traits of the RES covaried along two axes (Fig. 5a). The first axis opposed SRL and RD and represents the collaboration gradient related to the species' soil exploration strategy varying from a "do-it-yourself" acquisition strategy by roots that are efficient for soil exploration, to an "outsourcing" acquisition strategy via the investment of carbon in a mycorrhizal fungal partner for the return of limiting resources (Bergmann et al., 2020). The second axis is defined by RNC and RTD; it represents the conservation gradient opposing traits associated with high metabolic activity and traits associated with resource conservation in dense and long-living tissues. All mechanical traits increased with increasing SRL and decreasing root diameter. Such a result can be explained by the disparity of soil exploration strategy among species. Species adopting the "do-it-yourself" strategy may develop stronger and tougher roots to e.g. improve anchorage against grazing herbivores and facilitate soil penetration in compacted soils. On the other side of the axis, species adopting the

446 "outsourcing strategy" rely more on symbiotic partners to explore soil and acquire resources,
447 therefore a large investment in mechanical quality is less important for survival. This strategy
448 is especially true for species in the Fabaceae family that "collaborate" with both rhizobia and
449 arbuscular mycorrhizal fungi. For these species, roots are not solely responsible for the
450 exploration of soil volume, and nutrients are acquired by a large and complex fungi network.
451 Our results reinforce this hypothesis, as roots from species in the Fabaceae family were
452 mechanically weaker and less tough than those from individuals in the Poaceae family.

453 Surprisingly and in contrast with our expectations, the strength, stiffness and toughness of
454 *absorptive* roots generally decreased with increasing RTD. This result contrasts with those from
455 studies performed on roots of woody species (Ghestem et al. 2014; Yang et al. 2016; Boldin et
456 al. 2018). For herbaceous species, which have lower RTD than in roots from woody species
457 (Ma et al. 2018), our results suggest that mechanical properties are more driven by SRL and
458 RD than by RTD.In contrast to results for *absorptive* roots, we found that in *transport* roots,
459 the four fundamental traits of the RES covaried along a single axis of variation with SRL at one
460 end, and RD, RNC and RTD at the other end (Fig. 5b). The covariation of *transport* root traits
461 has, to our knowledge, never been studied, but it is not surprising that they did not follow the
462 RES found for *absorptive* roots since they have different functions. *Transport* roots are
463 composed of the highest root orders, and possess a high proportion of stele, indicating reduced
464 absorptive functionality but strong transportation capacity (McCormack et al. 2015). This
465 investment of biomass in structural dense tissue was also indicated by the positive relationship
466 between RD and RTD.

467 ***4.3 Interspecific variation of mechanical traits: and strong differences between monocots***
468 ***and dicots (H3)***

For both *absorptive* and *transport* roots, the first PCA axis strongly discriminated monocots and dicots. Monocots with higher SRL (i.e., with the "do-it-yourself" strategy), had stronger, tougher roots that deformed less under loading than dicot roots, with greater flexibility (ε_r) and a higher load/work to failure for the same cross-sectional area (T_r and W_r) (Figs. 2, 3 and 5), while dicots displaying higher RD, RNC and RTD (i.e., the outsourcing strategy) had weaker root mechanical quality. Only modulus of elasticity (E_r) was similar between monocot and dicot roots (Figs. 4, 6e and 6f). These results are not surprising, since monocots and dicots generally exhibit contrasting root development pattern, anatomy, morphology and chemical compositions. First, roots of monocots have higher SRL but lower diameter, tissue density and N concentration than dicots (Freschet et al. 2017). These differences are consistent with the absence of secondary growth in monocots, whereas in dicots the increase of secondary vascular tissue and the loss of cortex with increasing root orders cause an increase in diameter and root tissue density. The higher mechanical properties of monocots might thus result from: (i) their thinner diameter since we demonstrated that at the interspecific level mechanical traits (except E_r) are negatively correlated with RD and positively with SRL, (ii) their anatomy; despite roots of monocots lack secondary growth, their endoderm undergo a secondary cell wall thickening consisting in the development of suberin lamella and lignified cell-walls (Enstone et al., 2002; Ma and Peterson, 2003; Lux et al. 2004; Zhou et al. 2020) that might increase mechanical quality; (iii) their chemical composition; indeed in the same experiment, roots of monocots tended to possess higher (non-significant) cellulose and lignin concentrations than dicot roots (Rossi et al., 2020). As the two most important components of root cell walls, cellulose is a polysaccharide comprising a linear chain of glucose units, and lignin is a polymer made by cross-linking phenolic precursors (Genet et al. 2005; Zhang et al. 2014). Cellulose shapes the structured microfibrils in root cell walls, while lignin fills the spaces between the microfibrils and reinforces the cell wall, increasing root strength (Genet et al. 2005; Zhang et al. 2014).

494 However, results on the relationships between root cellulose, lignin and mechanical traits lack
495 a consensus in literature. For example, greater cellulose concentration was associated with
496 stronger (Genet et al. 2005), or weaker (Zhang et al. 2014; Zhu et al. 2020) roots, or had no
497 influence on strength (Hathaway and Penny 1975). Hathaway and Penny (1975) and Zhang et
498 al. (2014) found that lignin concentration was a better predictor of strength than cellulose
499 concentration. However, all these studies focused on woody species rather than herbaceous
500 plants and examined intraspecific patterns rather than interspecific patterns. The differences
501 between monocots and dicots revealed in this study need however to be investigated further
502 with more species since our results are possibly biased by the dicots selected that are mostly
503 dinitrogen-fixing, comprising species with roots that have a low tissue density and are rich in
504 nitrogen (Weigelt et al. 2021).

505

5 CONCLUSIONS

Using twelve herbaceous species from contrasting taxonomical families cultivated in a experimental garden, we found strong intra- and inter- specific variation of mechanical traits in *absorptive* and *transport* roots, and revealed their relationships with morphological and chemical traits related to root economics. Transport roots were usually stronger and tougher and deformed more than absorptive roots that are ephemeral in nature, and so shall require less investment for mechanical build-up than longer-lived *transport* roots. Mechanical traits were not or only weakly related to root locations. Monocot roots were stronger and tougher than dicot roots and had a greater capacity to withstand permanent deformation. As a pioneer study exploring the relationships between mechanical traits and other functional traits related to root economics, our study demonstrated that mechanical traits are a fundamental part of the root economics spectrum through a strong association with the 'do-it-yourself' soil exploration strategy. Species adopting the "do-it-yourself" acquisition strategy (i.e., thin roots with high SRL for efficient soil exploration), had stronger and tougher roots that would also improve anchorage and facilitate soil penetration. On the other side of the axis, species with an "outsourcing" acquisition strategy (i.e., with a greater investment of carbon in a mycorrhizal fungal partner for the return of limiting resources), invested less in mechanical quality. Given the importance of root mechanical integrity in plant anchorage, our results provide new evidence on the trade-off and synergy among organ multifunctionality, thus contributing to the mechanistic understanding of plant functioning.

It is worthwhile to mention that the investigated mechanical traits are related to a plant' ability of providing the ecosystem service of soil reinforcement and slope stabilization against natural hazards (Stokes et al. 2009; Ghestem et al. 2014). Our results are therefore useful for identifying candidate herbaceous plant species in ecological restoration.

ACKNOWLEDGEMENTS

(hidden)

REFERENCES

Bergmann, J. et al. 2020. The fungal collaboration gradient dominates the root economics space in plants. - Science Advances 6, eaba3756.

Boldrin, D. et al. 2017. Correlating hydrologic reinforcement of vegetated soil with plant traits during establishment of woody perennials. - Plant Soil 416: 437–451.

Boldrin, D. et al. 2018. Effects of root dehydration on biomechanical properties of woody roots of *Ulex europaeus*. - Plant Soil 431: 347–369.

Boldrin, D. et al. 2021. Root age influences failure location in grass species during mechanical testing. - Plant Soil in press.

Burylo, M. et al. 2011. Soil reinforcement by the roots of six dominant species on eroded mountainous marly slopes (Southern Alps, France). - CATENA 84: 70–78.

Chimungu, J. G. et al. 2015. Root anatomical phenes predict root penetration ability and biomechanical properties in maize (*Zea Mays*). - Journal of Experimental Botany 66: 3151–3162.

Cohen, D. et al. 2009. Fiber bundle model for multiscale modeling of hydromechanical triggering of shallow landslides. - Water Resources Research 45(10).

Cohen, D. et al. 2011. An analytical fiber bundle model for pullout mechanics of root bundles. - J. Geophys Res 116: F03010.

Daget, P. 1977. Le bioclimat méditerranéen : caractères généraux, modes de caractérisation. - Vegetatio 34 : 1–20.

de Baets, S. et al. 2008. Root tensile strength and root distribution of typical Mediterranean plant species and their contribution to soil shear strength. - Plant Soil 305: 207–226.

Dumlao, M. R. et al. 2015. The role of root development of *Avena fatua* in conferring soil strength. - American Journal of Botany 102: 1050–1060.

Ekeoma, E. C. et al. 2021. Drying of fibrous roots strengthens the negative power relation between biomechanical properties and diameter. - Plant Soil in press.

Enstone, D. E. et al. 2002. Root endodermis and exodermis: structure, function, and responses to the environment. - J Plant Growth Regul 21: 335–351.

Fan, C.-C. and Su, C.-F. 2008. Role of roots in the shear strength of root-reinforced soils with high moisture content. - Ecological Engineering 33: 157–166.

Felsenstein, J. 1985. Phylogenies and the comparative method. - The American Naturalist 125: 1–15.

Fitter, A. H. 1982. Morphometric analysis of root systems: application of the technique and influence of soil fertility on root system development in two herbaceous species. - Plant, Cell & Environment 5: 313–322.

Freschet, G. T. et al. 2017. Climate, soil and plant functional types as drivers of global fine-root trait variation. - Journal of Ecology 105: 1182–1196.

Freschet, G. T. et al. 2021. A starting guide to root ecology: strengthening ecological concepts and standardising root classification, sampling, processing and trait measurements. - New Phytologist: 150.

Genet, M. et al. 2005. The Influence of cellulose content on tensile strength in tree roots. - Plant Soil 278: 1–9.

Genet, M. et al. 2011. Linking carbon supply to root cell-wall chemistry and mechanics at high altitudes in *Abies georgei*. - Annals of Botany 107: 311–320.

Ghestem, M. et al. 2014. A framework for identifying plant species to be used as 'ecological engineers' for fixing soil on unstable slopes (V Magar, Ed.). - PLoS ONE 9: e95876.

Giadrossich, F. et al. 2017. Methods to measure the mechanical behaviour of tree roots: A review. - Ecological Engineering 109: 256–271.

Graves, S. et al. 2015. multcompView: visualizations of paired comparisons. R package version 0: 1–7.
Guerrero-Ramírez, N. R. et al. 2021. Global root traits (GRooT) database. - Global Ecology and Biogeography 30: 25–37.
Hathaway, R. L. and Penny, D. 1975. Root Strength in Some *Populus* and *Salix* Clones. - New Zealand Journal of Botany 13: 333–344.
Harrell Jr, F. E. 2019. Package 'hmisc'. CRAN 2018, 2019 : 235–236. https://cran.r-project.org/web/packages/Hmisc/index.html
Iversen, C. M. et al. 2017. A global Fine-Root Ecology Database to address below-ground challenges in plant ecology. - New Phytol 215: 15–26.
Ji, J. et al. 2020. Energy-based fibre bundle model algorithms to predict soil reinforcement by roots. - Plant Soil 446: 307–329.
Jin, Y. and Qian, H. 2019. V.PhyloMaker: an R package that can generate very large phylogenies for vascular plants. - Ecography 42: 1353–1359.
Loades, K. W. et al. 2015. Effect of root age on the biomechanics of seminal and nodal roots of barley (*Hordeum vulgare* L.) in contrasting soil environments. - Plant Soil 395: 253–261.
Lux, A., et al. 2004. Root cortex: structural and functional variability and responses to environmental stress. - Root Research 13: 117–131.
Ma, F. and Peterson, C. A. 2003. Current insights into the development, structure, and chemistry of the endodermis and exodermis of roots. - Can. J. Bot. 81: 405–421.
Ma, Z. et al. 2018. Evolutionary history resolves global organization of root functional traits. - Nature 555: 94–97.
Mao, Z. et al. 2012. Engineering ecological protection against landslides in diverse mountain forests: Choosing cohesion models. - Ecological Engineering 45: 55–69.
Mao, Z. et al. 2014. Evaluation of root reinforcement models using numerical modelling approaches. - Plant Soil 381: 249–270.
Mao, Z. et al. 2018. Mechanical traits of fine roots as a function of topology and anatomy. - Annals of Botany 122: 1103–1116.
Mao, Z. 2022. Root reinforcement models: classification, criticism and perspectives. - Plant Soil in press.
McCormack, M. L. et al. 2015. Redefining fine roots improves understanding of below ‐ ground contributions to terrestrial biosphere processes. - New Phytol 207: 505–518.
Meijer, G. J. 2021. A generic form of fibre bundle models for root reinforcement of soil. - Plant Soil in press.
Méndez-Alonzo, R. et al. 2013. Ecological variation in leaf biomechanics and its scaling with tissue structure across three Mediterranean-climate plant communities (N Anten, Ed.). - Funct Ecol 27: 544–554.
Niklas, K. J. et al. 2002. The biomechanics of *Pachycereus pringlei* root systems. - American Journal of Botany 89: 12–21.
Oksanen, J. et al. 2015. Vegan community ecology package: ordination methods, diversity analysis and other functions for community and vegetation ecologists. R package version : 2–3. https://CRAN.R-project.org/package=vegan
Onoda, Y. et al. 2011. Global patterns of leaf mechanical properties: Global patterns of leaf mechanical properties. - Ecology Letters 14: 301–312.
Pagès, L. 2016. Branching patterns of root systems: comparison of monocotyledonous and dicotyledonous species. - Ann Bot 118: 1337–1346.
Paradis, E. et al. 2004. APE: analyses of phylogenetics and evolution in R language. - Bioinformatics 20: 289 – 290.

R Core Team. 2021. R: A language and environment for statistical computing. R Foundation for Statistical Computing, Vienna, Austria. URL https://www.R-project.org/.
Read, J. and Stokes, A. 2006. Plant biomechanics in an ecological context. - American Journal of Botany 93: 1546–1565.
Rossi, L. M. W. et al. 2020. Pathways to persistence: plant root traits alter carbon accumulation in different soil carbon pools. - Plant Soil 452: 457–478.
Roumet, C. et al. 2016. Root structure-function relationships in 74 species: evidence of a root economics spectrum related to carbon economy. - New Phytol 210: 815–826.
Schumacher, I. et al. 2021. Defects in Cell Wall Differentiation of the Arabidopsis Mutant rol1-2 Is Dependent on Cyclin-Dependent Kinase CDK8. - Cells 10: 685.
Stokes, A. et al. 2009. Desirable plant root traits for protecting natural and engineered slopes against landslides. - Plant Soil 324: 1–30.
Timoshenko S. P. 1956. Strength of materials, part II, advanced theory and problems, D. Vol. 210, 3rd edn. New York: Van Nostrand Company.
Waldron, L. J. and Dakessian, S. 1981. Soil reinforcement by roots: calculation of increased soil shear resistance from root properties. - Soil science 132/ 427–435.
Weemstra, M. et al. 2016. Towards a multidimensional root trait framework: a tree root review. - New Phytol 211: 1159–1169.
Weigelt, A. et al. 2021. An integrated framework of plant form and function: the belowground perspective. - New Phytologist 232: 42–59.
Williamson, V. M. and Gleason, C. A. 2003. Plant–nematode interactions. - Current Opinion in Plant Biology 6: 327–333.
Wright, I. J. and Westoby, M. 2002. Leaves at low versus high rainfall: coordination of structure, lifespan and physiology. - New Phytol 155: 403–416.
Wright, I. J. et al. 2004. The worldwide leaf economics spectrum. - Nature 428: 821–827.
Yang, Y. et al. 2016. Effect of Root Moisture Content and Diameter on Root Tensile Properties (D Hui, Ed.). - PLoS ONE 11: e0151791.
Zhang, C.-B. et al. 2014. Why fine tree roots are stronger than thicker roots: The role of cellulose and lignin in relation to slope stability. - Geomorphology 206: 196–202.
Zhou, M. et al. 2022. Using anatomical traits to understand root functions across root orders of herbaceous species in temperate steppe. - New Phytologist in press.
Zhu, H. et al. 2015. Anomalous scaling law of strength and toughness of cellulose nanopaper. - Proc Natl Acad Sci USA 112: 8971–8976.
Zhu, J. et al. 2020. How does root biodegradation after plant felling change root reinforcement to soil? - Plant Soil 446: 211–227.

TABLE AND FIGURE CAPTIONS

Table 1 Root mechanical traits and intermediate metrics included in the study and their function and significance.

Table 2 Species, family and number of root samples used in mechanical tests.

Table 3 Intra- and interspecific variation of root mechanical traits for each species as a function of root type (*Transport* versus *Absorptive*) and root position (*Transport–Proximal* versus *Transport–Distal* and *Absorptive-Proximal* versus *Absorptive–Distal*).

Table 4 Pearson's correlation coefficients among root traits of all species for *absorptive* roots (a) and *transport* roots (b). Trait-based correlations are presented below the diagonal line, while phylogenetic-independent contrast (PIC)-based correlations are presented above the central diagonal. Significant correlations are in bold in coloured cells (***$P < 0.001$; **$P < 0.01$; *$P < 0.05$): green – significantly positive correlation; orange – significantly negative correlation.

Figure 1 Illustration of the root types and sampling locations in the root systems of dicots and monocots.

Figure 2 Root tensile strength (T_r) as a function of diameter (d). Symbols: coloured symbols represent data for the species under consideration (small purple symbols for *absorptive* roots; large green symbols for *transport* roots) and grey symbols in the background (for better viewing) represent data values for the remaining species. Text: blue – Poaceae species; brown – Plantaginaceae species; orange – Rosaceae species; red – Fabaceae species; grey – all species together. Curves: in each subplot, two curves of power law function are illustrated: the coloured curve represents the fit for the concerned species using all root samples; the grey curve represents the fit for all the species together; A (multiplier) and B (exponent) are the two parameters of the power law. NS – the value of the parameter not significant from zero (***$P < 0.001$; **$P < 0.01$; *$P < 0.05$). Note that R^2 are adjusted R^2 which could be mathematically negative. See Table 2 for the number of replicates.

Figure 3 Root tensile strain (ε_r) as a function of diameter (d). Symbols: coloured symbols represent data for the species under consideration (small purple symbols for *absorptive* roots; large green symbols for *transport* roots) and grey symbols in the background (for better viewing) represent data values for the remaining species. Text: blue – Poaceae species; brown – Plantaginaceae species; orange – Rosaceae species; red – Fabaceae species; grey – all species together. Curves: in each subplot, two curves of power law function are illustrated: the coloured curve represents the fit for the concerned species using all the root samples; the grey curve represents the fit for all the species together; A (multiplier) and B (exponent) are the two parameters of the power law. NS – the value of the parameter not significant from zero (***$P < 0.001$; **$P < 0.01$; *$P < 0.05$). Note that R^2 are adjusted R^2 which could be mathematically negative. See Table 2 for the number of replicates.

Figure 4 Root modulus of elasticity (E_r) as a function of diameter (d). Symbols: coloured symbols represent data for the species under consideration (small purple symbols for *absorptive* roots; large green symbols for *transport* roots) and grey symbols in the background (for better viewing) represent data values for the remaining species. Text: blue – Poaceae species; brown – Plantaginaceae species; orange – Rosaceae species; red – Fabaceae species; grey – all species together. Curves: in each subplot, two curves of power law function are illustrated: the coloured curve represents the fit for the concerned species using all the root samples; the grey curve represents the fit for all the species together; A (multiplier) and B (exponent) are the two parameters of the power law. NS – the value of the parameter not significant from zero (***$P < 0.001$; **$P < 0.01$; *$P < 0.05$). Note that R^2 are adjusted R^2 which could be mathematically negative. See Table 2 for the number of replicates.

Figure 5 Root toughness (W_r) as a function of diameter (d). Symbols: coloured symbols represent data for the species under consideration (small purple symbols for *absorptive* roots; large green symbols for *transport* roots) and grey symbols in the background (for better viewing) represent data values for the remaining species. Text: blue – Poaceae species; brown – Plantaginaceae species; orange – Rosaceae species; red – Fabaceae species; grey – all species together. Curves: in each subplot, two curves of power law function are illustrated: the coloured curve represents the fit for the concerned species using all the root samples; the grey curve represents the fit for all the species together; A (multiplier) and B (exponent) are the two parameters of the power law. NS – the value of the parameter not significant from zero (***$P < 0.001$; **$P < 0.01$; *$P < 0.05$). Note that R^2 are adjusted R^2 which could be mathematically negative. See Table 2 for the number of replicates.

Figure 6 Effect of species category (monocots versus dicots) on root mechanical traits for each combination of root functional type and sampling location for the 12 species. Error bars represent standard errors. Numbers beside the bars represent numbers of observations. Pairs of treatments: *Proximal* – monocot versus *Proximal* – dicot and *Distal* – monocot versus *Distal* – dicot. For each pair, letters represent the Student's t-test results at $P < 0.05$ between the dicots and the monocots; in case of significance, "a" represents the larger value, while "b" represents the smaller value.

Figure 7 Relationships between all root traits using principal component analysis for *absorptive* (a) and *transport* roots (b). Colours of convex hull polygons: light red – dicots; light blue – monocots. Colours of arrows: deep red – root mechanical traits; black – root morphological or chemical traits. Each point represents a species, the colour of which is family-dependent: blue – Poaceae species; brown – Plantaginaceae species; orange – Rosaceae species; red – Fabaceae species species names: Be – *Bromus erectus*; Dg – *Dactylis glomerata*; Fr – *Festuca rubra*; Lp – *Lolium perenne*; Pp – *Poa pratensis*; Lc – *Lotus corniculatus*; Ms – *Medicago sativa*; Ov – *Onobrychis viciifolia*; Tp – *Trifolium pratense*; Tr – *Trifolium repens*; Pl – *Plantago lanceolata*; Sm – *Sanguisorba minor*. Symbols and acronyms of traits: T_r – tensile strength; ε_r – tensile strain; E_r – modulus of elasticity; W_r – tensile toughness; RNC – root nitrogen concentration; RTD – root tissue density; SRL –specific root length; RD – mean root diameter.

SUPPLEMENTARY TABLE AND FIGURE CAPTIONS

Table S1 Intra- and inter-specific variation of root morphological and chemical traits for each species as a function of root type (*Transport* versus *Absorptive*).

Table S2 Intra- and inter-specific variation of tensile load required to cause root failure (F_r, in N) for each species as a function of root type (*Transport* versus *Absorptive*) and root position (*Transport–Proximal* versus *Transport–Distal* and *Absorptive-Proximal* versus *Absorptive–Distal*).

Figure S1 The tensile load (F_r) required to cause root failure as a function of diameter (d). Symbols: coloured symbols represent data for the species under consideration (small purple symbols for *absorptive* roots; large green symbols for *transport* roots) and grey symbols in the background (for better viewing) represent data values for the remaining species. Text: blue – Poaceae species; brown – Plantaginaceae species; orange – Rosaceae species; red – Fabaceae species; grey – all species together. Curves: in each subplot, two curves of power law function are illustrated: the coloured curve represents the fit for the concerned species using all the root samples; the grey curve represents the fit for all the species together; A (multiplier) and B

(exponent) are the two parameters of the power law. NS – the value of the parameter not significant from zero (***$P < 0.001$; **$P < 0.01$; *$P < 0.05$).

Figure S2 Interspecific variation of root mechanical traits for each species as a function of root functional type (*transport* versus *absorptive*). T_r – root tensile strength (in MPa); ε_r – root tensile strain (in %); E_r – root modulus of elasticity (in MPa); W_r – tensile toughness (in MJ m^{-3}). For *x*-axis (Species), species are ranged in family, in a descending order of mean T_r. Colours are blue – Poaceae species; red – Fabaceae species; brown – Plantaginaceae species; orange – Rosaceae species; species names: Be – *Bromus erectus*; Dg – *Dactylis glomerata*; Fr – *Festuca rubra*; Lp – *Lolium perenne*; Pp – *Poa pratensis*; Lc – *Lotus corniculatus*; Ms – *Medicago sativa*; Ov – *Onobrychis viciifolia*; Tp – *Trifolium pratense*; Tr – *Trifolium repens*; Pl – *Plantago lanceolata*; Sm – *Sanguisorba minor*. In each subplot, the capital letters represent the Tukey HSD test results at $P < 0.05$.

Figure S3 Linear regressions between the four mechanical traits and the four morphological and chemical traits at interspecific level. Before regressions, all the traits were in log-transformed with base 10. *y*-axis: T_r – root tensile strength (in MPa); ε_r – root tensile strain (in %); E_r – root modulus of elasticity (in MPa); W_r – root tensile toughness (in MJ m^{-3}); *x*-axis: RD – mean root diameter (mm); SRL – specific root length (m g^{-1}); RTD – root tissue density (g cm^{-3}); RNC – root nitrogen concentration (mg g^{-1}). In each subplot, a linear function was fit for each root type (absorptive *versus* transport). For each root type, all the monocots (square symbols) and dicots (triangle symbols) were used in the same regression. A solid line represents that the slope is significantly different from zero. When it is not the case, a dashed line is used. Levels of significance for intercept and slope: NS – the value of the parameter not significant from zero; *** – $P < 0.001$; ** – $P < 0.01$; * – $P < 0.05$.

TABLES

Table 1

Intermediate metrics	**Definition and calculation**	**Schemas**
Load to a root (F, N) (Schemas A)	Time-dependent longitudinal load continuously and progressively applied to a root. F is measured by the datalogger of the test machine. The curve of F versus displacement (L) is noted as: $F = f(L)$	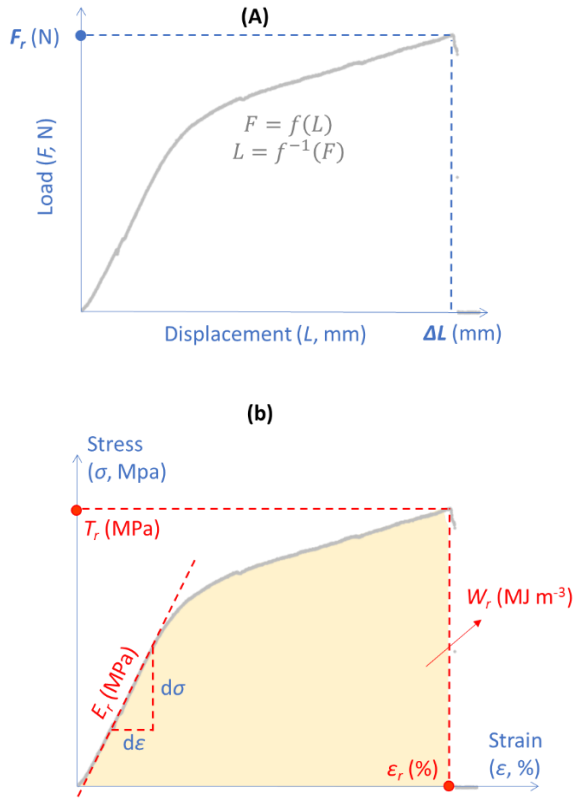
Root displacement (L, mm) (Schemas A)	Time-dependent absolute root deformation during a test. L is measured by the datalogger of the test machine. The curve of L versus load (F) is noted as: $L = f^{-1}(F)$	
Tensile load required to cause root failure (F_r, N) (Schemas A)	Maximum F, usually occurring at the root failure: $F_r = \max(F)$	
Ultimate root displacement (ΔL, mm) (Schemas A)	Root displacement when the maximum F occurs: $\Delta L = f^{-1}(F_r)$	
Root tensile stress (σ; MPa) (Schemas B)	Time-dependent tensile load per unit root cross sectional area: $\sigma = 4F/(\pi d^2)$ Where d is mean diameter of the root (mm). The curve of σ versus deformation (ε) is noted as: $\sigma = g(\varepsilon)$	
Root deformation/strain (ε, %) (Schemas B)	Relative longitudinal extension of a root during a test: $\varepsilon = \Delta L/L_0$ Where L_0 is initial length of the root sample (mm). The curve of ε versus tensile stress (σ) is noted as: $\varepsilon = g^{-1}(\sigma)$	
Traits	**Definition and calculation**	**Function and significance**
Root tensile strength (T_r, MPa) (Schemas B)	Maximum tensile load required per root cross-sectional area to cause failure of the root, either through breakage or nonreversible deformation: $T_r = \max(\sigma) = 4F_r/(\pi d^2)$	T_r represents root material's intrinsic ability of resistance to external forcing in tension. The higher T_r value that a root possesses, the stronger the root tissue is. A stronger root is able to mobilise higher strength when it is stretched out of soil, it thus improves plant anchorage and soil shear strength.

Root tensile strain (ε_r, %) (Schemas B)	Root deformation when the maximum T_r occurs: $$\varepsilon_r = g^{-1}(T_r)$$	ε_r reflects root material's intrinsic ability of deformation when being subject to external forcing. The higher ε_r value that a root possesses, the higher deformation the root tissue can reach before failure. Under perturbation, a root of higher ε_r may be more flexible against failure, but may also delay the root's efficacity to exert mechanical resistance.
Modulus of elasticity (E_r, MPa) (Schemas B)	Maximum slope of the quasi-linear part (elastic zone) of the relationship between σ and ε: $$E_r = \max(\frac{\mathrm{d}\sigma}{\mathrm{d}\varepsilon})$$	E_r reflects the root material's tensile elasticity or stiffness (Cohen et al. 2009; Ekeoma et al. 2021). The higher E_r value that a root possesses, the more elastic or stiffer the root tissue is. Generally, a stiffer root is able to withstand a higher load to elastically deform it under a given displacement, thus improving plant anchorage and provide greater soil reinforcement (Mao et al. 2014). Roots with large E_r can remain anchored in soil, even after soil failure has occurred, thus holding vegetation in place and retarding or preventing mass substrate failure (Freschet et al. 2021).
Root tensile toughness (W_r, MJ m^{-3}) (Schemas B)	Amount of energy per unit volume that a root can absorb before its fracture. W_r is calculated as the surface area of the curve of σ against ε: $$W_r = \int_0^{\varepsilon_r} f(\varepsilon)\mathrm{d}\varepsilon$$	W_r, also called deformation energy, represents the ability of a root to absorb energy without fracture and is an intrinsic mechanical quality of root tissue as a material by jointly considering strength and deformation (Ji et al. 2021). The higher W_r value that a root possesses, the tougher the root tissue is.

Note: In the schemas, the curve of σ against ε (in grey) is extracted from the mechanical test for one root sample (species: *Trifolium repens*, root type: *transport*; root location: *distal*; replicate no.: 3). Variables in red correspond to the traits used in plots and analyses, while variables in blue are intermediary metrics used to calculate the traits in red.

Table 2

Category	Family	Species	Abbreviation	Number of successful mechanical tests for root samples				Total
				Absorptive roots		*Transport* roots		
				Proximal	*Distal*	*Proximal*	*Distal*	
Monocot	Poaceae	*Bromus erectus*	Be	5	5	5	5	20
Monocot	Poaceae	*Dactylis glomerata*	Dg	3	4	5	4	16
Monocot	Poaceae	*Festuca rubra*	Fr	5	5	5	5	20
Monocot	Poaceae	*Lolium perenne*	Lp	5	5	5	5	20
Monocot	Poaceae	*Poa pratensis*	Pp	5	5	5	5	20
Dicot	Fabaceae	*Lotus corniculatus*	Lc	5	5	5	5	20
Dicot	Fabaceae	*Medicago sativa*	Ms	5	4	5	5	19
Dicot	Fabaceae	*Onobrychis viciifolia*	Ov	5	5	5	5	20
Dicot	Fabaceae	*Trifolium pratense*	Tp	5	3	4	5	17
Dicot	Fabaceae	*Trifolium repens*	Tr	5	5	5	5	20
Dicot	Plantaginaceae	*Plantago lanceolata*	Pl	5	4	5	5	19
Dicot	Rosaceae	*Sanguisorba minor*	Sm	5	5	5	5	20

Table 3

Trait	Species	*Absorptive*	*Transport*	*Absorptive-Proximal*	*Absorptive-Distal*	*Transport-Proximal*	*Transport-Distal*
T_r	Pp	**AC 25.32 ± 4.15 b**	**B 57.05 ± 12.67 a**	B 29.15 ± 6.81 a	A 21.49 ± 4.90 a	B 44.98 ± 6.54 a	B 69.11 ± 24.64 a
	Dg	A 26.93 ± 4.70 a	AB 44.74 ± 9.06 a	AB 23.94 ± 8.31 a	A 29.18 ± 6.23 a	AB 51.11 ± 11.17 a	AB 36.78 ± 15.70 a
	Lp	ABC 12.36 ± 3.72 a	AC 21.51 ± 11.68 a	AC 8.69 ± 2.77 a	A 16.04 ± 6.93 a	ABC 30.79 ± 22.32 a	A 12.23 ± 8.53 a
	Tr	BC 14.94 ± 2.15 a	AC 15.82 ± 1.40 a	C 13.41 ± 3.33 a	A 16.47 ± 2.94 a	ABC 15.23 ± 0.73 a	A 16.41 ± 2.85 a
	Fr	B 14.54 ± 3.45 a	C 15.27 ± 2.03 a	C 9.87 ± 2.56 a	A 19.22 ± 6.02 a	AC 17.30 ± 3.41 a	A 13.24 ± 2.20 a
	Tp	B 6.82 ± 2.73 a	C 12.50 ± 1.77 a	C 4.98 ± 1.40 a	A 11.39 ± 10.37 a	ABC 12.35 ± 2.01 a	A 12.62 ± 2.98 a
	Pl	**B 3.48 ± 0.35 b**	**C 10.61 ± 2.24 a**	C 3.54 ± 0.55 a	A 3.40 ± 0.46 a	**AC 15.20 ± 2.95 a**	**A 6.03 ± 1.85 b**
	Ms	B 7.81 ± 1.46 a	C 5.29 ± 0.50 a	**C 5.03 ± 1.35 b**	**A 11.29 ± 1.60 a**	C 5.33 ± 0.53 a	A 5.25 ± 0.92 a
	Ov	**B 3.49 ± 0.53 b**	**C 7.79 ± 0.61 a**	C 2.62 ± 0.70 a	A 4.35 ± 0.64 a	C 8.85 ± 0.65 a	A 6.74 ± 0.84 a
	Sm	B 3.92 ± 0.72 a	C 4.72 ± 1.27 a	C 3.62 ± 1.23 a	A 4.21 ± 0.89 a	C 5.97 ± 1.68 a	A 3.48 ± 1.90 a
	Be	**B 2.13 ± 0.28 b**	**C 5.57 ± 1.32 a**	C 2.65 ± 0.27 a	A 1.61 ± 0.39 a	C 8.11 ± 2.07 a	A 3.03 ± 0.62 a
	Lc	B 3.51 ± 1.04 a	C 3.47 ± 0.54 a	C 4.49 ± 1.99 a	A 2.54 ± 0.63 a	**C 4.54 ± 0.64 a**	**A 2.39 ± 0.58 b**
	All	**10.18 ± 1.02 b**	**16.83 ± 2.17 a**	8.83 ± 1.33 a	11.61 ± 1.54 a	18.41 ± 2.83 a	15.25 ± 3.30 a
ε_r	Fr	**AC 23.74 ± 4.21 b**	**B 40.18 ± 3.25 a**	B 21.42 ± 6.56 a	A 26.06 ± 5.83 a	B 43.20 ± 3.28 a	B 37.16 ± 5.68 a
	Pp	**A 20.90 ± 3.10 b**	**AB 37.89 ± 2.24 a**	AB 24.33 ± 4.42 a	A 17.47 ± 4.23 a	AB 38.13 ± 4.29 a	AB 37.65 ± 2.03 a
	Dg	ABC 24.70 ± 4.17 a	AC 31.58 ± 1.37 a	AC 27.72 ± 3.00 a	A 22.44 ± 7.24 a	ABC 30.45 ± 1.34 a	A 32.99 ± 2.67 a
	Lp	**BC 19.81 ± 3.52 b**	**AC 33.50 ± 2.12 a**	C 21.86 ± 5.44 a	A 17.77 ± 4.91 a	ABC 36.61 ± 1.54 a	A 30.40 ± 3.61 a
	Pl	**B 12.14 ± 1.57 b**	**C 25.10 ± 2.63 a**	C 13.76 ± 2.13 a	A 10.10 ± 2.17 a	**AC 31.03 ± 1.89 a**	**A 19.18 ± 3.17 b**
	Be	**B 10.32 ± 1.36 b**	**C 26.41 ± 5.00 a**	C 12.51 ± 1.86 a	A 8.14 ± 1.57 a	ABC 31.52 ± 8.88 a	A 21.31 ± 4.56 a
	Lc	**B 10.26 ± 2.26 b**	**C 18.26 ± 2.55 a**	C 14.25 ± 3.53 a	A 6.27 ± 1.61 a	AC 21.61 ± 2.37 a	A 14.91 ± 4.25 a
	Ov	**B 11.05 ± 1.25 b**	**C 16.55 ± 1.98 a**	C 9.60 ± 1.69 a	A 12.51 ± 1.77 a	C 19.86 ± 2.11 a	A 13.24 ± 2.78 a
	Tr	**B 8.60 ± 1.70 b**	**C 18.70 ± 1.86 a**	C 11.12 ± 2.31 a	A 6.07 ± 2.11 a	C 22.15 ± 0.97 a	A 15.24 ± 2.93 a
	Tp	**B 10.01 ± 2.45 a**	**C 16.20 ± 2.11 a**	C 9.54 ± 2.53 a	A 11.20 ± 7.72 a	C 16.11 ± 1.99 a	A 16.27 ± 3.70 a
	Ms	B 9.44 ± 1.09 a	C 13.19 ± 1.75 a	**C 7.59 ± 1.21 b**	**A 11.76 ± 1.22 a**	C 12.94 ± 1.67 a	A 13.44 ± 3.31 a
	Sm	**B 7.76 ± 1.46 b**	**C 13.92 ± 2.19 a**	C 8.26 ± 2.35 a	A 7.26 ± 1.97 a	C 15.56 ± 2.46 a	A 12.29 ± 3.76 a
	All	**13.85 ± 0.89 b**	**24.30 ± 1.11 a**	14.73 ± 1.23 a	12.93 ± 1.29 a	**26.78 ± 1.53 a**	**21.82 ± 1.55 b**

E_r	Dg	AC 251.23 ± 41.76 a	B 535.16 ± 164.65 a	B 226.53 ± 85.06 a	A 269.75 ± 47.12 a	B 660.21 ± 231.32 a	B 378.85 ± 242.54 a
	Pp	A 303.92 ± 46.24 a	AB 442.96 ± 126.51 a	AB 319.99 ± 62.44 a	A 287.86 ± 74.79 a	AB 313.74 ± 57.42 a	AB 572.18 ± 245.72 a
	Tr	ABC 362.14 ± 61.04 a	AC 322.25 ± 24.69 a	AC 273.69 ± 89.11 a	A 450.59 ± 70.10 a	ABC 299.51 ± 17.09 a	A 344.98 ± 46.82 a
	Lp	BC 246.65 ± 101.14 a	AC 218.00 ± 124.40 a	C 125.73 ± 65.22 a	A 367.56 ± 185.65 a	ABC 291.15 ± 231.60 a	A 144.86 ± 115.42 a
	Tp	B 138.10 ± 48.56 a	C 217.39 ± 26.54 a	C 136.12 ± 60.34 a	A 143.06 ± 114.38 a	AC 235.47 ± 36.12 a	A 202.92 ± 40.43 a
	Fr	B 163.84 ± 62.30 a	C 122.79 ± 17.64 a	C 98.04 ± 28.78 a	A 229.63 ± 120.29 a	ABC 131.83 ± 29.47 a	A 113.76 ± 22.15 a
	Ms	B 145.20 ± 33.32 a	C 118.29 ± 15.67 a	C 101.54 ± 40.00 a	A 199.78 ± 46.97 a	AC 130.74 ± 21.31 a	A 105.84 ± 23.95 a
	Sm	**B 154.95 ± 38.96 a**	**C 52.40 ± 12.18 b**	C 181.14 ± 79.33 a	A 128.76 ± 13.92 a	C 62.04 ± 18.75 a	A 42.76 ± 16.43 a
	Ov	**B 58.79 ± 11.52 b**	**C 144.98 ± 13.66 a**	C 45.44 ± 10.52 a	A 72.14 ± 19.94 a	C 165.18 ± 18.81 a	A 124.79 ± 16.80 a
	Pl	B 58.98 ± 15.06 a	C 109.87 ± 20.05 a	C 41.87 ± 11.47 a	A 80.36 ± 29.44 a	**C 152.71 ± 19.38 a**	**A 67.02 ± 22.69 b**
	Lc	B 84.18 ± 20.72 a	C 51.02 ± 6.84 a	C 75.39 ± 18.91 a	A 92.96 ± 39.18 a	**C 67.53 ± 7.28 a**	**A 34.50 ± 4.61 b**
	Be	B 38.69 ± 5.28 a	C 57.38 ± 7.40 a	C 45.10 ± 7.35 a	A 32.27 ± 7.13 a	C 68.25 ± 9.59 a	A 46.51 ± 9.77 a
	All	168.16 ± 16.45 a	196.38 ± 23.54 a	**136.21 ± 18.10 b**	**201.86 ± 27.33 a**	214.51 ± 33.42 a	178.24 ± 33.28 a
W_r	Pp	**AC 3.19 ± 0.81 b**	**B 13.43 ± 3.49 a**	B 4.38 ± 1.35 a	A 2.01 ± 0.67 a	B 10.49 ± 2.47 a	B 16.37 ± 6.65 a
	Dg	**A 4.01 ± 1.35 b**	**AB 8.49 ± 1.57 a**	AB 3.62 ± 0.86 a	A 4.30 ± 2.45 a	AB 9.87 ± 2.09 a	AB 6.76 ± 2.39 a
	Fr	ABC 2.12 ± 0.85 a	AC 3.74 ± 0.69 a	AC 1.05 ± 0.37 a	A 3.19 ± 1.58 a	ABC 4.47 ± 1.00 a	A 3.00 ± 0.92 a
	Lp	BC 1.35 ± 0.58 a	AC 4.19 ± 2.31 a	C 1.02 ± 0.24 a	A 1.67 ± 1.19 a	ABC 6.27 ± 4.44 a	A 2.12 ± 1.44 a
	Tr	**B 0.64 ± 0.18 b**	**C 2.02 ± 0.30 a**	C 0.71 ± 0.25 a	A 0.57 ± 0.28 a	AC 2.30 ± 0.15 a	A 1.74 ± 0.60 a
	Pl	**B 0.18 ± 0.03 b**	**C 1.88 ± 0.49 a**	C 0.22 ± 0.05 a	A 0.14 ± 0.03 a	**ABC 2.97 ± 0.62 a**	**A 0.78 ± 0.32 b**
	Tp	**B 0.52 ± 0.32 a**	**C 1.36 ± 0.27 a**	C 0.27 ± 0.16 a	A 1.16 ± 1.15 a	AC 1.37 ± 0.39 a	A 1.35 ± 0.41 a
	Be	B 0.11 ± 0.03 a	C 1.07 ± 0.44 a	C 0.16 ± 0.03 a	A 0.07 ± 0.03 a	C 1.70 ± 0.80 a	A 0.45 ± 0.13 a
	Ov	**B 0.17 ± 0.03 b**	**C 0.87 ± 0.15 a**	C 0.12 ± 0.03 a	A 0.23 ± 0.02 a	**C 1.17 ± 0.13 a**	**A 0.58 ± 0.19 b**
	Ms	B 0.38 ± 0.10 a	C 0.49 ± 0.10 a	**C 0.15 ± 0.03 b**	**A 0.67 ± 0.11 a**	C 0.49 ± 0.09 a	A 0.49 ± 0.20 a
	Lc	B 0.27 ± 0.16 a	C 0.43 ± 0.09 a	C 0.47 ± 0.32 a	A 0.07 ± 0.03 a	**C 0.60 ± 0.10 a**	**A 0.26 ± 0.10 b**
	Sm	B 0.13 ± 0.04 a	C 0.54 ± 0.20 a	C 0.11 ± 0.04 a	A 0.16 ± 0.08 a	C 0.65 ± 0.21 a	A 0.44 ± 0.37 a
	All	**1.03 ± 0.18 b**	**3.18 ± 0.51 a**	0.93 ± 0.21 a	1.14 ± 0.29 a	3.57 ± 0.62 a	2.79 ± 0.80 a

Note: In the column “Trait”: T_r – root tensile strength (in MPa); ε_r – root tensile strain (in %); E_r – root modulus of elasticity (in MPa); W_r – root tensile work (in MPa). In the column “Species,” for each trait, species are ranged in a descendent order according to the average of all the tested roots of the concerned trait (not shown); colours: blue – Poaceae species; red – Fabaceae species; brown – Plantaginaceae species; orange – Rosaceae species; species names: Be – *Bromus erectus*; Dg – *Dactylis glomerata*; Fr – *Festuca rubra*; Lp – *Lolium perenne*; Pp – *Poa pratensis*; Lc – *Lotus corniculatus*; Ms – *Medicago sativa*; Ov – *Onobrychis viciifolia*; Tp – *Trifolium pratense*; Tr – *Trifolium repens*; Pl – *Plantago lanceolata*; Sm – *Sanguisorba minor*. Data are mean ± standard error. Statistical results for intraspecific variation: data in bold and in grey background highlight the significant cases according to the Student's t-test, each of which was performed for a pair of data (*Transport* versus *Absorptive*, *Transport–proximal* versus *Transport–Distal* and *Absorptive–proximal* versus *Absorptive–Distal*) for each species; the lower case letters after the values represent the Student's t-test results at $p < 0.05$; in case of significance, “a” represents the larger value, while “b” represents the smaller value. Statistical results for interspecific variation: the capital letters before the values represent the Tukey HSD test results at $p < 0.05$ across species for each of the six types of roots.

Table 4

(a) Absorptive roots

Trait category	Trait		T_r	ε_r	E_r	W_r	RD	SRL	RTD	RNC	C:N
Mechanical traits	Tensile strength	T_r		**0.63***	**0.78****	**0.93*****	-0.46	**0.86*****	**-0.65***	0.14	0.05
	Tensile strain	ε_r	**0.68***		0.22	**0.80****	-0.08	0.51	-0.34	-0.33	0.51
	Modulus of elasticity	E_r	**0.89*****	0.36		**0.80****	-0.08	0.51	-0.34	-0.33	0.51
	Tensile work	W_r	**0.96*****	**0.84*****	**0.76****		-0.33	**0.72***	-0.52	-0.00	0.19
Morphological and chemical traits	Mean root diameter	RD	**-0.61***	**-0.58***	-0.55	**-0.62***		**-0.69***	**0.64***	-0.15	-0.18
	Specific root length	SRL	**0.74****	**0.61***	**0.69***	**0.74****	**-0.97*****		**-0.83****	0.12	0.15
	Root tissue density	RTD	**-0.80****	-0.42	**-0.81****	**-0.78****	0.42	**-0.64***		-0.53	0.19
	Root nitrogen concentration	RNC	-0.12	**-0.60***	0.05	-0.24	**0.67***	-0.49	-0.25		**-0.88*****
	Carbon to nitrogen ratio	C:N	0.16	**0.62***	0.00	0.28	**-0.71***	0.54	0.19	**-1.00*****	

(b) Transport roots

Trait category	Trait		T_r	ε_r	E_r	W_r	RD	SRL	RTD	RNC	C:N
Mechanical traits	Tensile strength	T_r		0.37	**0.91*****	**0.98*****	-0.05	0.24	-0.05	-0.25	0.54
	Tensile strain	ε_r	**0.71****		0.12	0.48	-0.20	**0.88*****	-0.09	-0.22	**0.70***
	Modulus of elasticity	E_r	**0.91*****	0.42		**0.82****	-0.17	-0.05	-0.23	-0.33	0.44
	Tensile work	W_r	**0.97*****	**0.85*****	**0.81****		-0.01	0.40	0.03	-0.24	0.58
Morphological and chemical traits	Mean root diameter	RD	-0.50	-0.70*	-0.35	**-0.59***		-0.27	**0.88*****	0.59	-0.09
	Specific root length	SRL	**0.64***	**0.95*****	0.35	**0.79****	**-0.79****		-0.05	-0.34	0.51
	Root tissue density	RTD	-0.45	**-0.81****	-0.22	**-0.59***	**0.77****	**-0.89*****		0.39	0.02
	Root nitrogen concentration	RNC	-0.57	**-0.76****	-0.24	**-0.69***	0.54	**-0.80****	**0.58***		-0.58
	Carbon to nitrogen ratio	C:N	0.57	**0.77****	0.25	**0.70***	-0.54	**0.81****	**-0.59***	**-1.00*****	

Notes: Colours: green – positive and significant correlation ; orange – negative and significant correlation. Significance code: ***$P < 0.001$; **$P < 0.01$; *$P < 0.05$.

FIGURES

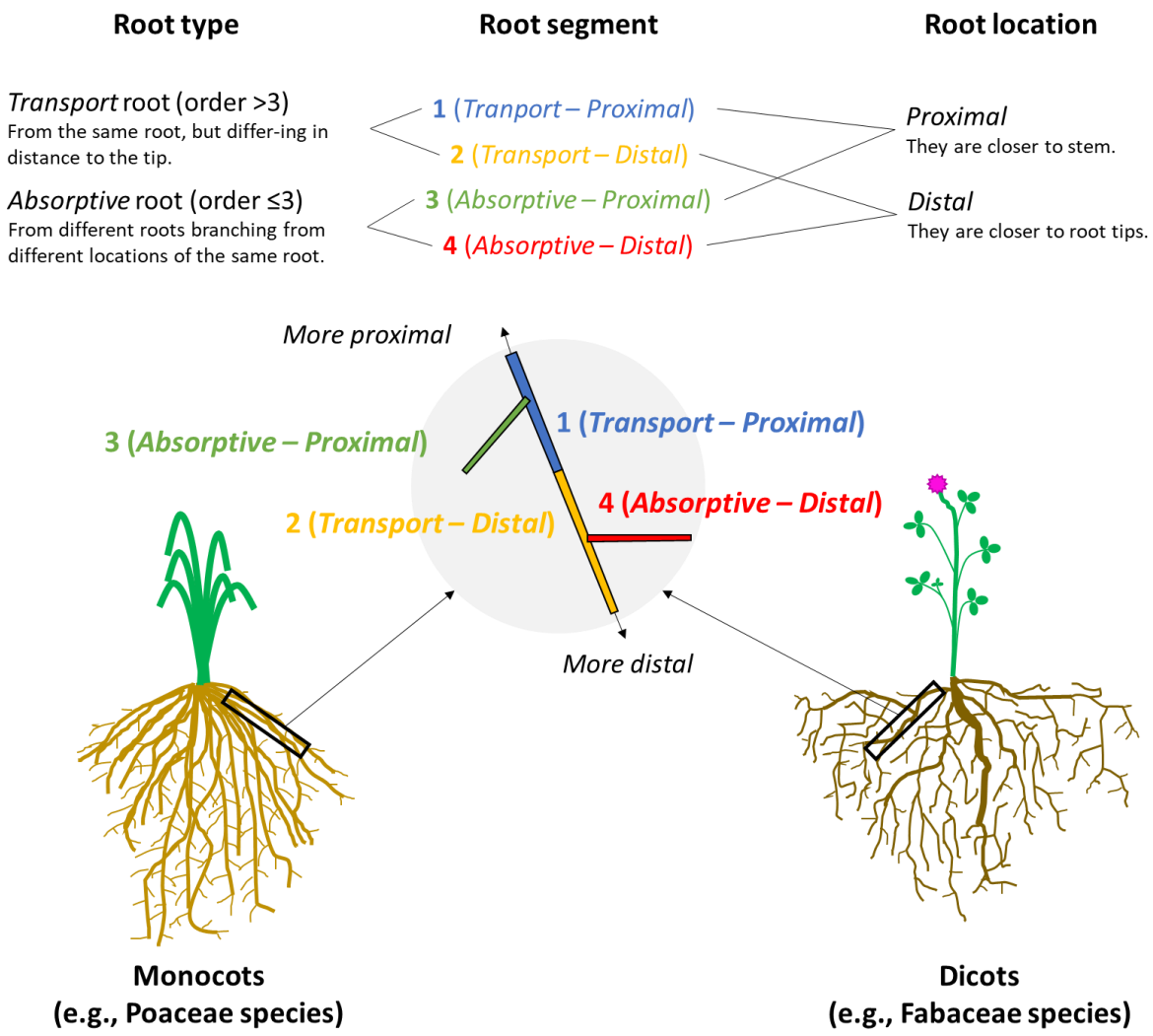

Figure 1

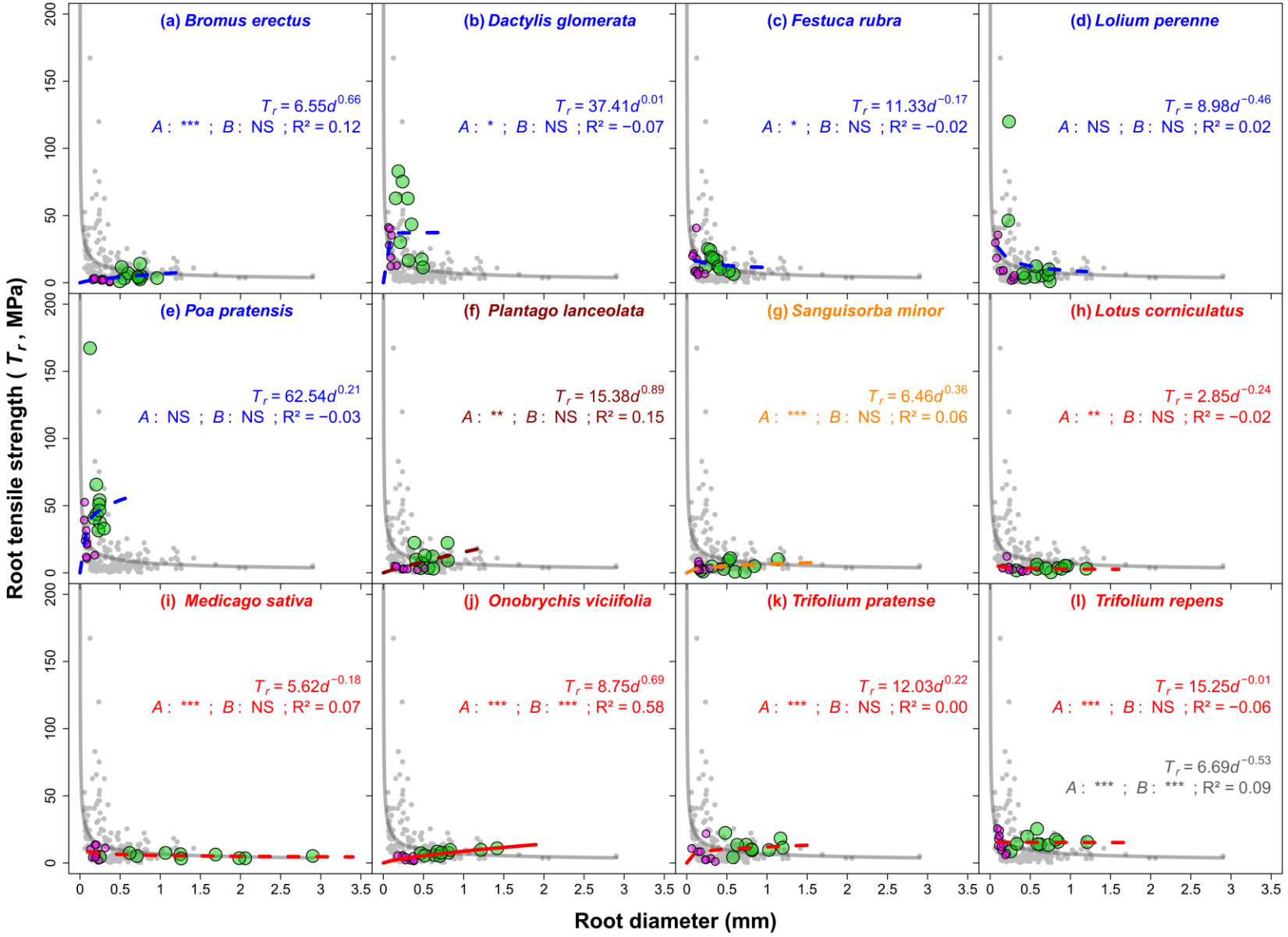
(a) Bromus erectus
$T_r = 6.55d^{0.66}$
A : *** ; B : NS ; R² = 0.12
(b) Dactylis glomerata
$T_r = 37.41d^{0.01}$
A : * ; B : NS ; R² = −0.07
(c) Festuca rubra
$T_r = 11.33d^{-0.17}$
A : * ; B : NS ; R² = −0.02
(d) Lolium perenne
$T_r = 8.98d^{-0.46}$
A : NS ; B : NS ; R² = 0.02
(e) Poa pratensis
$T_r = 62.54d^{0.21}$
A : NS ; B : NS ; R² = −0.03
(f) Plantago lanceolata
$T_r = 15.38d^{0.89}$
A : ** ; B : NS ; R² = 0.15
(g) Sanguisorba minor
$T_r = 6.46d^{0.36}$
A : *** ; B : NS ; R² = 0.06
(h) Lotus corniculatus
$T_r = 2.85d^{-0.24}$
A : ** ; B : NS ; R² = −0.02
(i) Medicago sativa
$T_r = 5.62d^{-0.18}$
A : *** ; B : NS ; R² = 0.07
(j) Onobrychis viciifolia
$T_r = 8.75d^{0.69}$
A : *** ; B : *** ; R² = 0.58
(k) Trifolium pratense
$T_r = 12.03d^{0.22}$
A : *** ; B : NS ; R² = 0.00
(l) Trifolium repens
$T_r = 15.25d^{-0.01}$
A : *** ; B : NS ; R² = −0.06
$T_r = 6.69d^{-0.53}$
A : *** ; B : *** ; R² = 0.09
Root tensile strength (T_r , MPa)
Root diameter (mm)
0
50
100
150
200
0.5
1
1.5
2
2.5
3
3.5

Figure 2

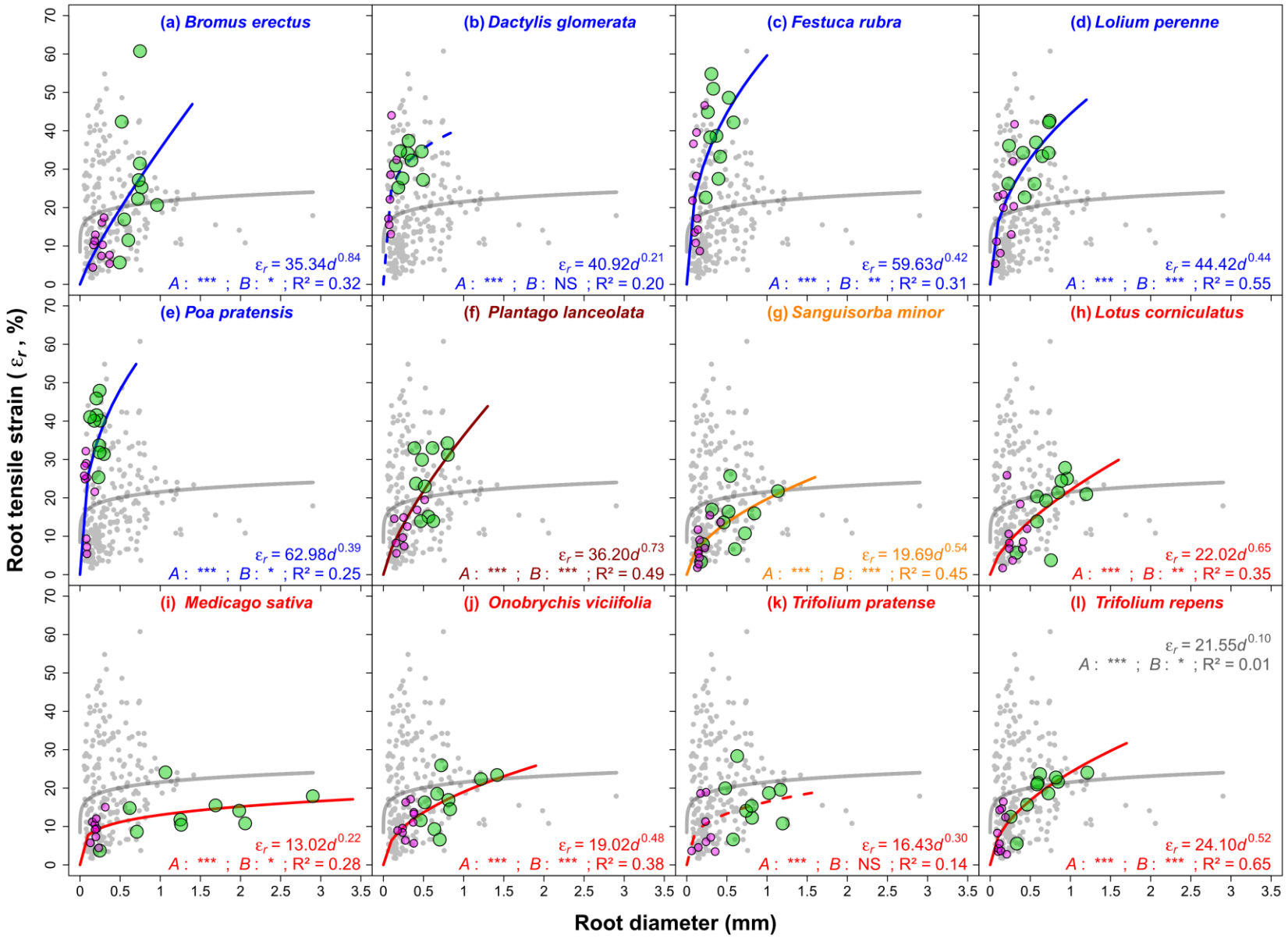
(a) Bromus erectus
εr = 35.34d^0.84
A : *** ; B : * ; R² = 0.32
(b) Dactylis glomerata
εr = 40.92d^0.21
A : *** ; B : NS ; R² = 0.20
(c) Festuca rubra
εr = 59.63d^0.42
A : *** ; B : ** ; R² = 0.31
(d) Lolium perenne
εr = 44.42d^0.44
A : *** ; B : *** ; R² = 0.55
(e) Poa pratensis
εr = 62.98d^0.39
A : *** ; B : * ; R² = 0.25
(f) Plantago lanceolata
εr = 36.20d^0.73
A : *** ; B : *** ; R² = 0.49
(g) Sanguisorba minor
εr = 19.69d^0.54
A : *** ; B : *** ; R² = 0.45
(h) Lotus corniculatus
εr = 22.02d^0.65
A : *** ; B : ** ; R² = 0.35
(i) Medicago sativa
εr = 13.02d^0.22
A : *** ; B : * ; R² = 0.28
(j) Onobrychis viciifolia
εr = 19.02d^0.48
A : *** ; B : *** ; R² = 0.38
(k) Trifolium pratense
εr = 16.43d^0.30
A : *** ; B : NS ; R² = 0.14
(l) Trifolium repens
εr = 21.55d^0.10
A : *** ; B : * ; R² = 0.01
εr = 24.10d^0.52
A : *** ; B : *** ; R² = 0.65
Root tensile strain (εr , %)
Root diameter (mm)
0 10 20 30 40 50 60 70
0 0.5 1 1.5 2 2.5 3 3.5

Figure 3

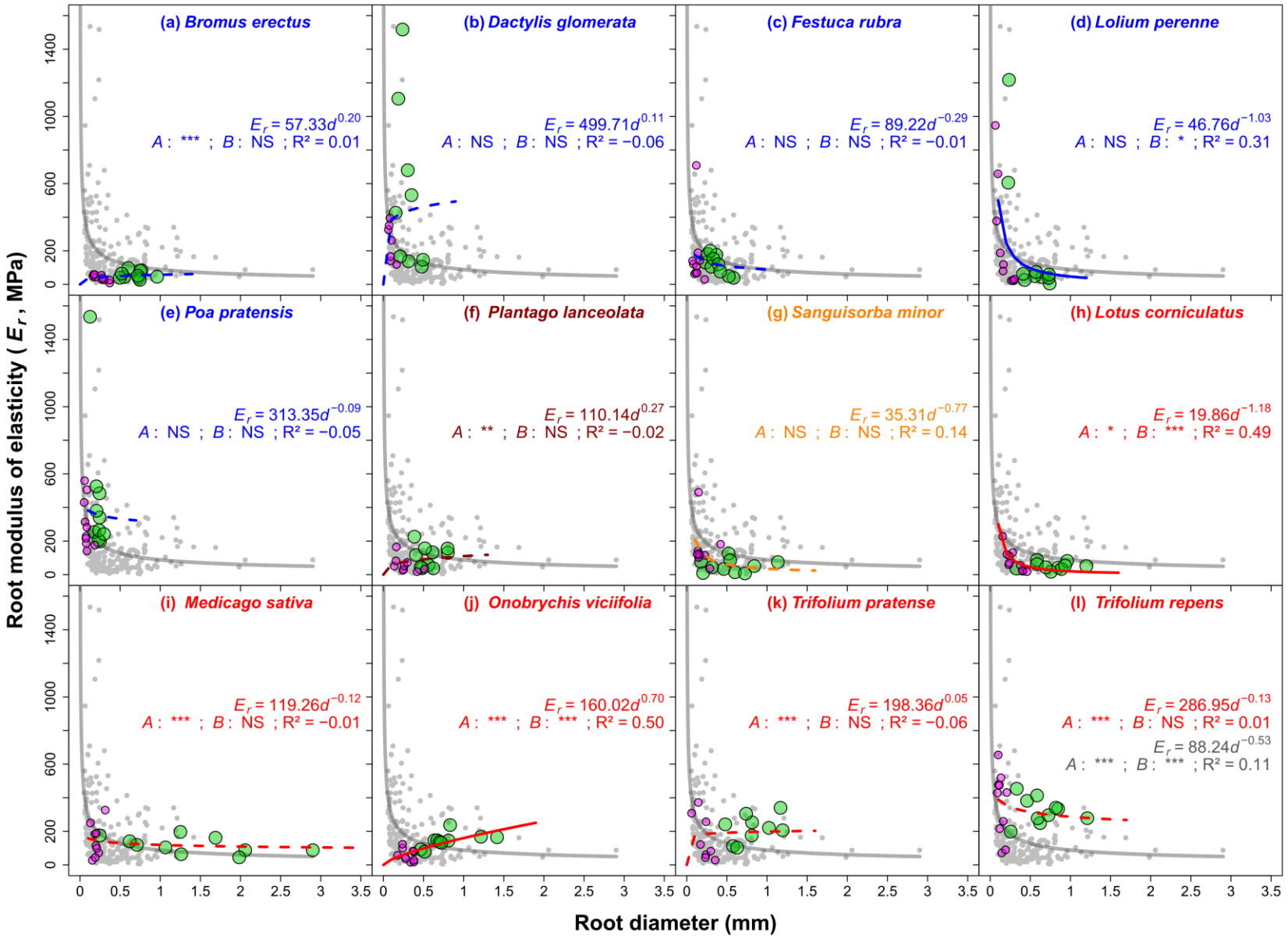
(a) Bromus erectus
$E_r = 57.33d^{0.20}$
A : *** ; B : NS ; R² = 0.01
(b) Dactylis glomerata
$E_r = 499.71d^{0.11}$
A : NS ; B : NS ; R² = −0.06
(c) Festuca rubra
$E_r = 89.22d^{-0.29}$
A : NS ; B : NS ; R² = −0.01
(d) Lolium perenne
$E_r = 46.76d^{-1.03}$
A : NS ; B : * ; R² = 0.31
(e) Poa pratensis
$E_r = 313.35d^{-0.09}$
A : NS ; B : NS ; R² = −0.05
(f) Plantago lanceolata
$E_r = 110.14d^{0.27}$
A : ** ; B : NS ; R² = −0.02
(g) Sanguisorba minor
$E_r = 35.31d^{-0.77}$
A : NS ; B : NS ; R² = 0.14
(h) Lotus corniculatus
$E_r = 19.86d^{-1.18}$
A : * ; B : *** ; R² = 0.49
(i) Medicago sativa
$E_r = 119.26d^{-0.12}$
A : *** ; B : NS ; R² = −0.01
(j) Onobrychis viciifolia
$E_r = 160.02d^{0.70}$
A : *** ; B : *** ; R² = 0.50
(k) Trifolium pratense
$E_r = 198.36d^{0.05}$
A : *** ; B : NS ; R² = −0.06
(l) Trifolium repens
$E_r = 286.95d^{-0.13}$
A : *** ; B : NS ; R² = 0.01
$E_r = 88.24d^{-0.53}$
A : *** ; B : *** ; R² = 0.11
Root modulus of elasticity (E_r , MPa)
Root diameter (mm)
0
200
600
1000
1400
0.5
1
1.5
2
2.5
3
3.5

Figure 4

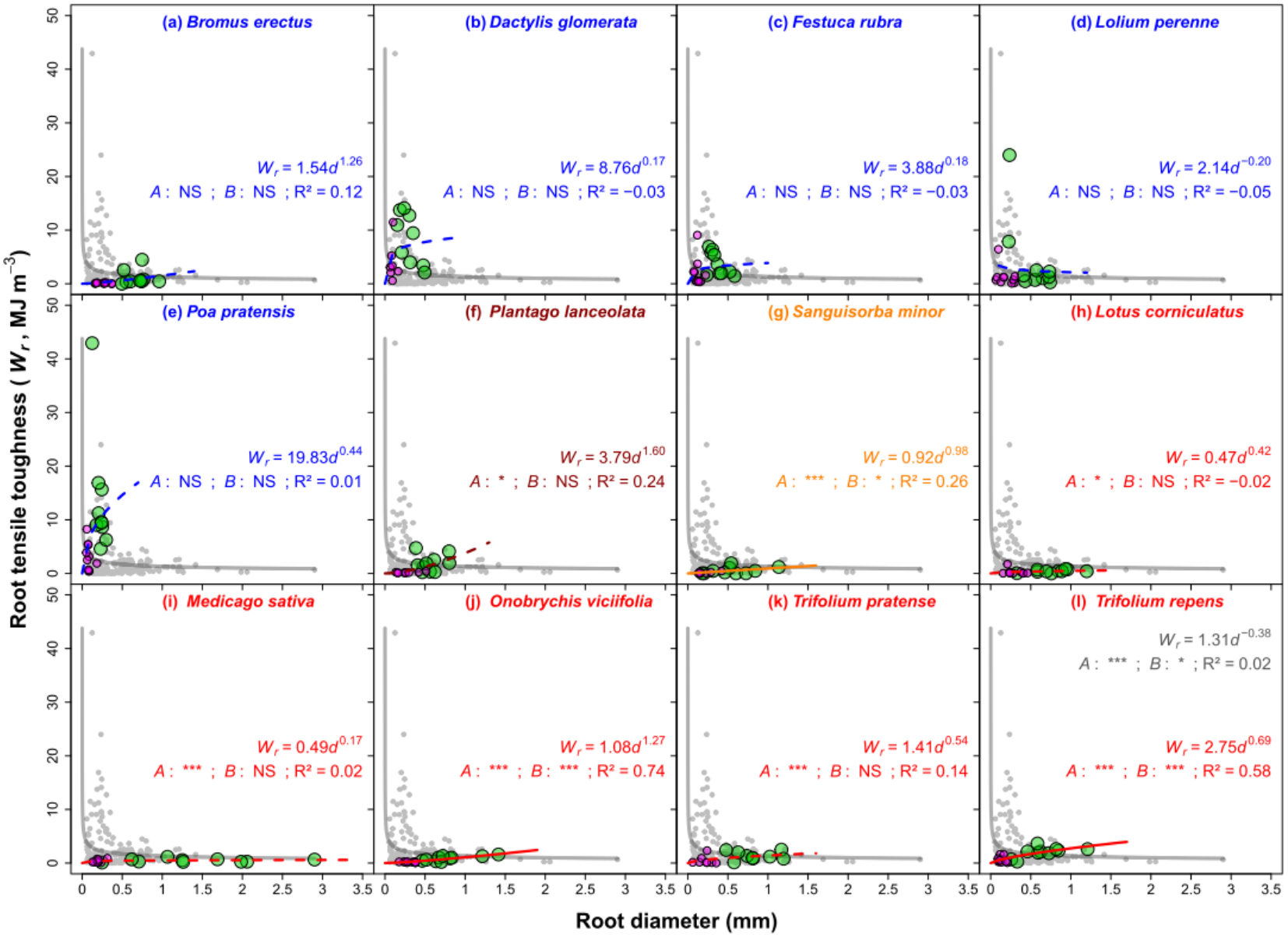
(a) Bromus erectus
$W_r = 1.54d^{1.26}$
A : NS ; B : NS ; R² = 0.12
(b) Dactylis glomerata
$W_r = 8.76d^{0.17}$
A : NS ; B : NS ; R² = −0.03
(c) Festuca rubra
$W_r = 3.88d^{0.18}$
A : NS ; B : NS ; R² = −0.03
(d) Lolium perenne
$W_r = 2.14d^{-0.20}$
A : NS ; B : NS ; R² = −0.05
(e) Poa pratensis
$W_r = 19.83d^{0.44}$
A : NS ; B : NS ; R² = 0.01
(f) Plantago lanceolata
$W_r = 3.79d^{1.60}$
A : * ; B : NS ; R² = 0.24
(g) Sanguisorba minor
$W_r = 0.92d^{0.98}$
A : *** ; B : * ; R² = 0.26
(h) Lotus corniculatus
$W_r = 0.47d^{0.42}$
A : * ; B : NS ; R² = −0.02
(i) Medicago sativa
$W_r = 0.49d^{0.17}$
A : *** ; B : NS ; R² = 0.02
(j) Onobrychis viciifolia
$W_r = 1.08d^{1.27}$
A : *** ; B : *** ; R² = 0.74
(k) Trifolium pratense
$W_r = 1.41d^{0.54}$
A : *** ; B : NS ; R² = 0.14
(l) Trifolium repens
$W_r = 1.31d^{-0.38}$
A : *** ; B : * ; R² = 0.02
$W_r = 2.75d^{0.69}$
A : *** ; B : *** ; R² = 0.58
Root tensile toughness (W_r , MJ m^{-3})
Root diameter (mm)
0 10 20 30 40 50
0 0.5 1 1.5 2 2.5 3 3.5

Figure 5

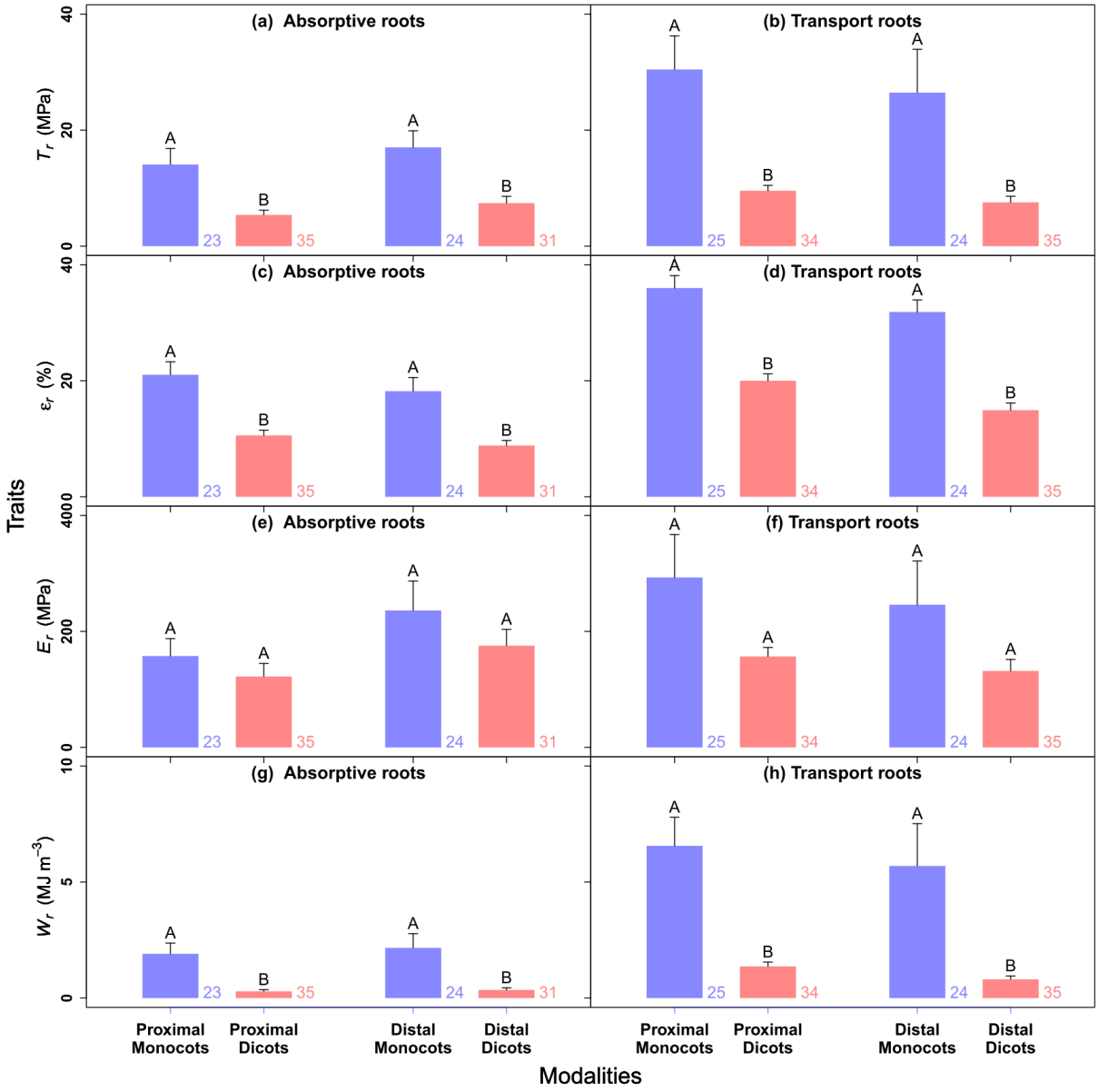
(a) Absorptive roots
(b) Transport roots
(c) Absorptive roots
(d) Transport roots
(e) Absorptive roots
(f) Transport roots
(g) Absorptive roots
(h) Transport roots
Traits
T_r (MPa)
ε_r (%)
E_r (MPa)
W_r (MJ m^{-3})
Proximal Monocots
Proximal Dicots
Distal Monocots
Distal Dicots
Modalities

Figure 6

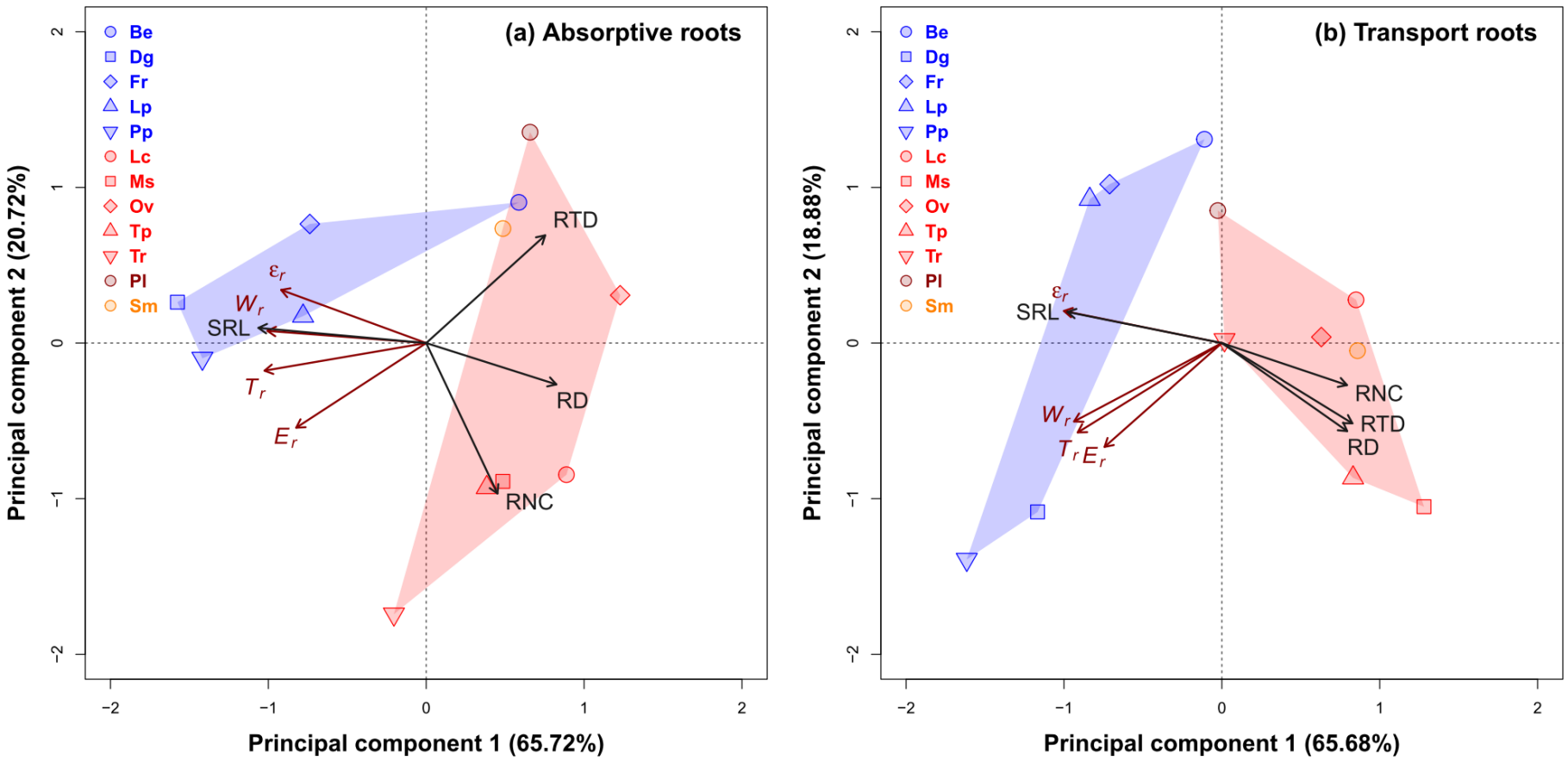
(a) Absorptive roots
(b) Transport roots
Be
Dg
Fr
Lp
Pp
Lc
Ms
Ov
Tp
Tr
Pl
Sm
RTD
RD
RNC
SRL
ε_r
W_r
T_r
E_r
Principal component 1 (65.72%)
Principal component 2 (20.72%)
Principal component 1 (65.68%)
Principal component 2 (18.88%)

Figure 7